Empirical support for the biogeochemical niche hypothesis in forest trees

Empirical support for the Biogeochemical Niche Hypothesis in forest trees

Sardans[1,2], J., Vallicrosa[1,2], H., Zuccarini[1,2], P. Farré-Armengol[1,2] G., Fernández-Martínez[3], M., Peguero[1,2], G., Gargallo-Garriga[1,2], A., Ciais[4] P., Janssens[3] I.A., Obersteiner[5] M., Richter[6], A., Peñuelas[1,2], J.

[1] CSIC, Global Ecology Unit CREAF-CEAB-UAB, Bellaterra, 08193 Catalonia, Spain.

[2] CREAF, Cerdanyola del Vallès, 08193 Catalonia, Spain.

[3] PLECO (Plants and Ecosystems), Department of Biology, University of Antwerp, B-2610 Wilrijk, Belgium.

[4]Laboratoire des Sciences du Climat et de l'Environnement, IPSL, 91191 Gif-sur-Yvette, France.

[5]International Institute for Applied Systems Analysis (IIASA), Ecosystems Services and Management, Schloss platz 1, A-2361 Laxenburg, Austria.

[6] University of Vienna, Terrestrial Ecosystem Research, Department of Microbiology and Ecosystem Science, 1090 Vienna, Austria

The possibility of using the elemental compositions of species as a tool to identify species/genotype niche remains to be tested at a global scale. We investigated the relationships between the foliar elemental compositions (elementomes) of trees at a global scale with phylogeny, climate, N deposition and soil traits. We analyzed foliar N, P, K, Ca, Mg and S concentrations in 25544 trees of 227 species. Shared ancestry explained 60-94% of the total variance of foliar nutrient concentrations and ratios, whereas current climate, atmospheric N deposition and soil type together explained 1-7%, consistent with the biogeochemical niche (BN) hypothesis that expects each species to have a specific need and use of each bioelement. The remaining variance was explained by the avoidance of nutritional competition with other species and the natural variability within species. The BN hypothesis is thus able to quantify species-specific tree niches and their shifts in response to environmental changes.

The "niche" theory is fundamental to ecology, because niches are both drivers and consequences of evolutionary processes[1-4]. The concept is easy to understand theoretically: each species tends to occupy a particular position along the gradients of all abiotic and biotic variables that define and determine fitness. This view is consistent with the niche concepts defined by Tracy and Christian (1986)[1], Wright et al. (2006)[5] and Swanson et al. (2015)[6], among many others, where the niche is directly associated with a multivariate space. Accurately measuring the exact parameters of a niche, however, is challenging due to the large number of variables that affect organisms within ecosystems. Several approaches have been developed in recent decades to more easily manage this complex and multivariate concept, e.g. niche regeneration[7] and functional niche[8-10]. A more general and easier method for defining and measuring species niches using field data, however, is needed.

The recently proposed Biogeochemical Niche (BN) hypothesis[11-13] incorporates most, if not all, niche parameters using species-specific elemental composition and stoichiometry. The assumptions underlying this hypothesis are based on the idea that each species is a unique genetic pool of individuals, a product of long-term evolutionary processes, so each species should have a specific morphological structure and functionality (from gene expression to physiological processes). Fundamental biological processes (e.g. growth, secondary metabolism, reproduction and storage of bio-elements) have distinct rates in different species, depending on selection pressures, so different species must differentially allocate elements to various traits of tissues and organs. Each species should thus tend to have its own elemental composition and stoichiometry (homeostatic component of BN). The changing circumstances during the lives of organisms, however, should also determine a necessary phenotypical plasticity to allow the individuals of each species to adapt its functionality and morphology during their lives (plasticity component). This ability differs in extent and quality among species. BN plasticity depends on the current genotypic and thus

genetic variability of a population and also on the phenotypical plasticity of individuals to respond to environmental shifts throughout their lives. The BN hypothesis allows us to detect plasticity at two levels: within populations due to the intraspecific variability in elemental composition of a set of individuals of the same species living under the same environmental conditions at a specific time (e.g. due to individual genotypic differences or different ontogenetic stages), and at the individual level (phenotypic plasticity) by indicating how each individual of a population varies its elemental composition when environmental conditions shift[13].

The BN hypothesis is useful for representing the ecological niche of each species in a hyper-dimensional volume generated by different bio-elemental concentrations and stoichiometric relationships, which could be simply and practically tested by a combined chemical and mathematical approach using multivariate and phylogenetic analyses[13]. The position of each species in the hyper-dimensional volume can shift with time and changing environmental conditions depending on the degree of species-specific stoichiometric plasticity (plasticity component), but the BN should also tend to maintain its own identity relative to the BNs of other species (homeostatic component)[13]. BN space at a specific time should therefore be a consequence of historical and current trends toward maximizing fitness in response to abiotic and biotic circumstances such as trophic relationships and water, light or nutrient availabilities and fluxes[13-15]. The various levels of plasticity among species can be detected because homeostatic species will occupy a smaller volume in multi-dimensional space, and plastic species will occupy a larger volume[13]. For example, comparing the movement/expansion/contraction of the BNs of two populations of different species or genotypes submitted to the same environmental shifts will thus provide information about their levels of BN plasticity[13]. The temporal shifts of the BN of a species or population can also be calculated, so we can follow the signatures of evolution on the BN. BNs also allow us to describe and quantify the expansion, contraction and extinction of niches and the appearance of new niches (e.g. when new species colonize an ecosystem)[13]. The BN hypothesis, however, has been experimentally tested only at small spatial and phylogenetic scales[11-17].

We aimed to test the BN hypothesis in forest trees across all forest biomes and continents (**Fig. S1**). Our study was based on the elementome of leaves, the plant organ where most compounds (from those allocated to growth or reproduction to those allocated to energy metabolism, defense or storage) are synthesized and where photosynthesis, the most crucial plant function, occurs. Leaves thus constitute a key organ in plant functioning, and we can define the 'species biogeochemical niche' for each species in its environmental circumstances by analyzing changes in foliar elemental composition. We built a global data set to test the extent to which (i) shared ancestry, (ii) abiotic factors (e.g. climate, N deposition and soil traits) and (iii) biotic factors (e.g. composition of the community inhabited by a tree) affect the BN. We hypothesized that each species would have a different need and use for each bio-element to optimize function and thus that shared ancestry would account for a large part of the foliar elemental composition in a wide set of data from a broad spectrum of species. Species, however, also evolve to some degree during fluctuating environmental conditions, so some of the variability of elemental composition should be due to

the phenotypic component and thus to current abiotic and biotic conditions such as climate, soil type, atmospheric N deposition and competition, which should account for another part of the variability of elemental composition. We thus expected to demonstrate the suitability of using the elemental compositions of organisms, the "elementome"[13], to define species-specific "niche differences" in a tangible and measurable way, providing a new valuable tool for establishing and identifying species niches.

Results

Phylogeny and BN size

The analysis of Pagel's λ identified significant phylogenetic signals in foliar N, P, K, S, Ca and Mg concentrations, N:Ca, N:Mg, P:Ca, P:Mg, P:S, K:Ca and K:S ratios and the scores of the first six PCA axes (**Table S1, Figs. 1-4 a**nd **S2-S14**) *, with Pagel's λ values in several variables >0.5.* These variables tended to be more similar in the clades of more recently separated species than in the clades of more phylogenetically distant species, thus demonstrating that the divergence of the values of the variables among the clades over time were largely and significantly driven by evolutionary processes. For example, foliar N concentrations were more similar among Pinaceae species than between Pinaceae and Fagaceae species, with Pinaceae species generally having lower values than Fagaceae species (**Fig. 1**). The phylogenetic signals using Pagel's λ were generally more similar in the subset of the database that also contained information for foliar C concentrations (7479 datapoints representing 138 species) than in the general database without foliar C concentrations (**Tables S2 and S3**, **Figs. S15-S19).** Of the 33 variables studied, only the foliar C:K ratio did not have a significant λ. Furthermore, these Pagel's λ values were high, >0.6, for most of the nutrient variables (**Table S2**).

The range of values in a functional discriminant analysis (FDA) (mainly along Root 1 that explained 90.8% of the total variance) that represented the sizes of species-specific BNs was larger for the species subjected to lower climatic stress (*Quercus robur* and *Q. petraea*) than for Mediterranean species adapted to drought (*Pinus halepensis*, *P. pinaster* and *Q. ilex*) (**Fig. 5**, **Tables S4 and S5**). These five species were the most abundant in our survey and were clearly separated in the multivariate space by significant distances (squared Mahalanobis distances) (**Table S4**) and in all foliar variables that significantly contributed to the separation of all species (**Table S5**). We also detected a strong phylogenetic effect in the distribution of scores along the first three root axes of the FDA (**Table S6**).

Abiotic factors

Climate, N deposition and soil type.

Phylogeny explained most of the variance of the foliar elemental compositions. Phylogeny explained 58.7-91.7% (mean 80.9%) of the variance of the foliar concentrations of the six bio-elements, 39.0-94.1% (mean 68.8%) of the variance in their pairwise ratios and 43.2-89.6 (mean 74.0%) of the variance in the scores of the first three axes of a principal component analysis (PCA) (**Table S7**). Species explained 1.4-14.6% (mean 5.58%) of the variance of the foliar concentrations of the six bio-elements, 0.4-28.1% (mean 8.1%) of the variance in pair-wise ratios and 0.6-13.8% (mean 5.07%) of the variance in the scores of thefirst three PC scores. Inheritance thus explained 73.3-93.6% (mean 86.5%) of the variance in the foliar concentrations of the six bio-elements, 67.1-94.5% (mean 81.7%) of the variance in their pairwise ratios and 57-90.2% (mean 79.1%) of the variance in the scores of the first three PC .

The climatic variables and N deposition, independently from their effect on current species distribution, explained 0.43-4.2% (mean 2.26%) of the variance in the foliar concentrations of the six bio-elements, 0.27-7.4% (mean 5.05%) of the variance in their ratios and 0.35-11.0% (mean 4.23%) of the variance in the scores of the first three PC (**Table S7**). Mean annual precipitation (MAP) and mean annual temperature (MAT) were the most important climatic variables explaining the variances of the elemental concentrations, with some relevant exceptions. For example, the variability of foliar N concentration was partially due to positive correlations with MAP, MAT, N deposition and mean annual solar radiation (**Table S6**). Interestingly, MAT and mean solar radiation had contrasting relationships with MAP and N deposition on overall foliar elemental composition, as indicated by the PC1 scores (**Table S7**).

Higher precipitation was associated with lower foliar concentrations of metal elements (K, Ca and Mg) and P and was positively correlated with foliar N and S concentrations (**Table S7**). MAT was correlated positively with foliar N and metal (K, Ca, Mg) concentrations and N:P ratio and negatively with foliar P concentrations. N deposition was correlated positively with foliar N, P and S concentrations and negatively with foliar Ca, Mg and K concentrations.

Soil type explained a low percentage of the variances in elemental compositions and ratios (**Table S8**), ranging between 0.1% in the foliar P:S ratio to 2.0% in foliar K concentrations. A PCA, however, indicated that trees growing in different soil types occupied significantly different areas of the 2D plot of the first two PC axes (**Fig. 6**) and that this distribution was mainly explained by phylogeny (R^2 = 0.72, 0.84 and 0.87 for the PC1, PC2 and PC3 scores, respectively) (**Table S8**). Trees growing on Inceptisols and Alfisols, typical of temperate forests, occupied a central position in this space. Trees growing in Alfisols, typical of wet and mesic temperate forests, had intermediate foliar N and K concentrations and the second highest foliar P concentration (**Fig. S20**), with intermediate ratios of foliar N:P, N:K and P:K (**Fig. S21**). Trees growing in Spodosols, very common in boreal and alpine coniferous forests, had the highest P and lowest K foliar concentrations (**Fig. S20**) and thus the highest foliar P:K ratios (**Fig. S21**). Trees growing in Oxisols, typical of wet tropical forests, had the second highest foliar N concentrations and the lowest foliar P concentrations (**Fig. S20**), the highest foliar N:P and N:K ratios and the lowest foliar P:K ratio (**Fig. S21**).

Biotic factors

Competition of foliar elementomes between coexisting species.

Foliar N and P concentrations, the N:P ratio and the scores for the first two PCA axes for species frequently shifted significantly when the distributions of two species overlapped. These differences usually explained little of the variance of the foliar variables, but they were statistically significant (**Tables S9-S15**). For example, foliar N and P concentrations, the N:P ratio and the scores for the first two PCA axes differed significantly when *P. abies* grew in areas with and without *Q. robur* (**Fig. S22a**), although the percentage of explained variance was ≤3.5% (**Table S9**). These shifts were reciprocal. Foliar P concentrations, N:P ratios and the PC1 scores also differed significantly between subsets of *Q. robur* growing in areas with and without *P. abies* (**Fig. S22a**, **Table S10**), explaining a maximum of only 5% of the total variance. Foliar P concentrations, N:P ratios and the PC1 scores differed significantly between *A. alba* coexisting or not with *Q. petraea* (**Fig. S22b**, **Table S11**), explaining a maximum of 5% of the total variance, and foliar N and P concentrations, N:P ratios and the PC1 scores differed significantly between *Q. petraea* coexisting or not with *A. alba* (**Table S12**), explaining a maximum of 4% of the total variance. Foliar N concentrations and the PC1 scores differed significantly between *Fagus sylvatica* growing in areas with and without *P. sylvestris* (**Fig. S22c**, **Table S13**), explaining a maximum of 2% of the total variance. Foliar N and P concentrations, N:P ratios and the PC1 scores differed significantly between *P. sylvestris* growing in areas with and without *F. sylvatica* (**Fig. S22c**, **Table S14**), explaining a maximum of 1% of the total variance. The percentage of variance explained for some of the variables was much higher in some cases, e.g. 17% for the foliar N concentration of *P. sylvestris* growing with or without *Q. robur* (**Table S14**) and 35% for the foliar P concentration of *Larix decidua* growing with or without *Q. robur* (**Table S15**).

Discussion

BN size and phylogeny

The use of the foliar concentrations of several bio-elements clearly separated the species in the hypervolume generated by the corresponding multivariate analyses, as previously reported only in smaller studies[11-18]. The FDA plot (showing 95.8% of the total explained variance) clearly separated the BNs of the species, with *Pinus* species having positive values on Root 1 and *Quercus* species having more negative values, also consistent with the positive link between phylogenetic distance and species-specific BN identity among species.

N, P, K, S, Ca and Mg contribute differentially to plant metabolic and physiological functions and to cells, tissues and organs. We therefore expected that different species, as evolutionary products, would have different optimal elemental compositions (elementomes)[11-14]. The results of our analysis of the global set of 227 of the most representative tree species worldwide (163, 58 and 6 from tropical, temperate and boreal biomes, respectively) strongly support this hypothesis. The results also indicated that the foliar BNs of the species became more similar as their phylogenetic distance decreased. These results are fully consistent with Kerkhoff et al.[19], who also found a consistent and significant phylogenetic signal in N and P

concentrations in plant organs in a set of 1287 plant species. The small number of published studies of BNs, all including fewer species, have also reported significant organ or body stoichiometric dependence on taxonomy and/or phylogeny of plant and animal species, although not all studies detected links between species phylogeny and N:P ratios[20]. The great majority of the studies nevertheless found significant relationships between species elemental composition and taxonomic and phylogenetic distance[20]. Similar results have also been obtained in ionomic studies[21].

Phylogeny and species, as proxies of overall genomic difference, however, did not explain 100% of the variability in the elementome. Some of the phylogenetic lines of distant clades may have been exposed to similar environmental conditions that would have driven parallel selection of the characteristics that determine elemental concentrations, consequently eliciting convergence to more similar elementomes than would be expected from their phylogenetic distance. In other words, species that are phylogenetically distant (e.g. that have developed on different continents but under current similar environmental conditions) may occupy a similar BN. For example, a change toward a warmer climate can increase the speed of evolution of several characters differently in different species[5,22,23]. Several other factors, such as species migration, changes of species interactions (e.g. with herbivorous or parasitic species) and climatic convergence can increase the speed of evolutionary convergence among species in different clades[24-26]. Distant clades could thus evolve under new, more similar, environmental conditions, favoring a trend toward convergence in functionality and thus in elementome. The results nevertheless indicated that evolutionary processes have significantly contributed to the differences in foliar elementomes that originated during species diversification, directly explaining 57-94.5% (averaging 85.7%) of the variance of their foliar concentrations and ratios. Anacker and Strauss (2016)[27] also recently reported that the niche differences among species increased with phylogenetic distance, again consistent with our results. Part of the inheritability factor that differs from phylogeny explained an average of about 7% of the variance of the variables studied, perhaps due to the recent divergent evolution of more proximal taxonomical species recently adapting to distinct and divergent environmental shifts in their respective distribution areas. .

Climate and N deposition

Several studies have reported trends in foliar N and P concentrations and N:P ratios in trees growing along climatic and latitudinal gradients[28-31], but their results have not always fully agreed. Most studies have observed a general trend toward decreasing foliar and litter P concentrations and increasing N:P ratios as latitude decreased and MAT, MAP and length of growing season increased[28-34]. Not all studies, however, have detected clear patterns of N:P ratios among or within the climatic areas[33]. Townsend et al. (2007)[34] and Lovelock et al. (2007)[35], for example, found no relationship between the N:P ratio and either latitude or MAP in tropical areas. Even when a significant relationship was detected in these studies, climatic variables explained only a small fraction of the variation in foliar elements, e.g. 16-25 and 5-35% reported by Yuan and Chen (2009)[31] and Reich and Oleksyn (2004)[28], respectively, depending on the variable. These studies used linear models that considered only climatic variables and N deposition without

phylogeny and species as random factors. The variance explained by climatic variables in our study decreased in our Bayesian analyses when we added species as a random factor (0.3-11.0%, with a mean of 4.3% among all variables) (**Table S6**).

Our results thus indicated significant relationships of foliar nutrient composition with N deposition and basic climatic traits such as MAP and MAT at a global scale. A decrease in foliar P concentrations and an increase in foliar N concentrations and N:P ratios with increasing MAT are consistent with the frequently observed higher N and lower P concentrations in plants toward equatorial latitudes. We also identified a general and significant relationship of the foliar concentrations of the main macronutrients with N deposition. The lower foliar metal concentrations with higher levels of N deposition are completely consistent with the higher leaching of soil bases associated with N deposition and with the bases competition for plant absorption with ammonium[36]. The higher foliar N and S concentrations with more N deposition are also due to the consequent higher availability of soil N and S[37,38]. Interestingly, we also identified a global positive correlation between higher levels of N deposition and higher foliar P concentrations when local studies reported all types of results, from increases to decreases in foliar P concentrations. The increases in P concentrations have been associated with higher capacities of plants and microbes to mobilize and take up more P due to higher N availability[39,40]. Lower foliar P concentrations under higher N loads, however, have been associated with a stronger P limitation[41-43]. Our results thus indicated that N deposition in forests at the global scale tends to increase foliar P concentrations but also N:P ratios, thus generally trending toward more P-limited forests.

Soil type

Soil type explained a modest but significant amount of the variance (0.1-2%) of tree foliar composition and stoichiometry. In fact, soil type and its capacity to supply some of the most important bio-elements to plants are partially due to historic and current climatic conditions. Species foliar elementomes were consistent with the traits of the various soil types (**Fig. 6**). Trees growing in Inceptisols and Alfisols, typical of temperate forests, occupied a central position in the PCA space, suggesting a more balanced elemental composition than trees growing in other soil types. Trees growing in Andisols and Vertisols, two soil types rich in easily weathered minerals such as Ca^{2+} and Mg^{2+}[44,45], typically had higher than average foliar Ca and Mg concentrations. Andisols are volcanic soils that are frequently rich in Fe-Mg silicates and in anorthite, a Ca feldspar. Ertisols are characterized by high concentrations of expandable clays, such as vermiculite and montmorillonite that are also rich in Mg and Ca, respectively. Trees growing in Spodosols (typical of sandy soils) had the lowest concentrations of Ca, Mg and K, which could be linked with the high leaching of basic cations in these acidic soils and consequently the low content of exchangeable complexes and slow mineralization. Trees growing in Spodosols also had the highest foliar P concentrations (**Fig. S15**) and thus the highest foliar P:K ratios. Trees growing in Oxisols (wet tropical forests) had the second highest foliar N concentrations, the lowest foliar P concentrations, the highest foliar N:P and N:K ratios and the lowest

foliar P:K ratio (**Fig. S16**). These results for Oxisols were consistent with recent observations of low foliar P concentrations and high foliar N:P ratios in wet tropical forests[28,32]. To the best of our knowledge, our global study is the first to associate high foliar N:K and low foliar P:K ratios with wet tropical forests. Relationships between foliar BN and soil type along natural gradients have recently been observed[46], but these relationships may not be as strong as expected and may not necessarily be universal. Ordoñez et al. (2009)[29] observed that the concentrations of some elements and ratios were correlated between soil type and photosynthetic tissues but others were not.

Competition among coexisting species

The foliar N and P concentrations, the N:P ratio and the scores for the first two PCA axes for species shifted significantly when the distributions of two species overlapped. These differences usually explained little of the variance of the foliar elemental concentrations and ratios but were significant (**Tables S8-S14**). For example, foliar N and P concentrations, the N:P ratio and the scores for the first two PCA axes differed significantly when *P. abies* grew in areas with and without *Q. robur*, although the percentage of explained variance was ≤3.5% (**Table S8**). These shifts were reciprocal and occurred for the pairs of the tree species, which were the most dominant in Europe (**Tables S8-S14**). These results of field analyses are consistent with the results of an experiment in seminatural grasslands where the target species shifted their elemental compositions depending on the neighboring species[17].

Homeostasis versus plasticity

Intraspecific variability explained a significant amount (2-20%) of the total random variability of all elemental concentrations and ratios (**Tables S6 and S7**). Species that have evolved in highly fluctuating environments are expected to have a larger capacity of functional and/or morphological shifts and thus require a more plastic stoichiometry than species that have evolved in a more stable environment[13,39]. Our results confirmed these expectations: the range of values in the FDA that represented the sizes of species-specific BNs was larger (P<0.001 along Roots 1 and 2) for the species subjected to less climatic stress (*Q. robur* and *Q. petraea*) than for the Mediterranean species adapted to drought (*P. halepensis*, *P. pinaster* and *Q. ilex*) (**Fig. 5**, **Tables S5 and S6**). These results indicated a trade-off between adaptation to being competitive in a stable environment versus being successful in a more fluctuating environment. Different levels of environmental stress cause a continuum of strategies between homeostasis and plasticity. Species growing in more stressful environments, with poor resource availability, have less BN plasticity than species growing in less stressful and richer environments[47,48].

Conclusions

The results of this study provide clear support for the BN hypothesis[13]. First, each species had a different BN, with a significant trend of larger differences in BNs as phylogenetic distance and evolutionary time increased. Recent evolutionary convergence due, for example, to recent adaptation of distant clades to

similar soil or climatic environments, however, indicated that the differences in BN among species could not be fully resolved by phylogenetic analyses alone. Second, environmental factors such as climate and soil type also explained an important part of the intraspecific variance in BN. These effects were moderate but significant and independent of taxonomy. Each species could be represented by its specific space in the hypervolume generated by the multivariate analysis of its foliar elemental composition and stoichiometry (elementome), so its specific plasticity was observed in the shift of its space in response to environmental changes. Third, coexisting competing species tended to have distinct BNs to minimize competitive pressure. Fourth, a trade-off between adaptations to being competitive in a stable environment versus being successful in a more fluctuating environment generated a continuum of strategies between homeostasis and plasticity.

METHODS

Data acquisition

Foliar Data. We gathered 25 544 datapoints of foliar N, P, K, Ca, Mg and S concentrations, expressed as percent dry weight. These data corresponded to 227 tree species at a global scale, including all latitudes and ecosystems. We only considered tree species with more than three locations. The data were obtained from 192 publications (Table S1) and inventories such as the Catalan Forest Inventory[49]. We also gathered and used a subset of 7479 datapoints with 138 species that contained information of foliar C concentration, in addition to foliar N, P, K, Mg, Ca and S concentrations, for identifying possible differences in the analyses with or without C concentrations. All data had been obtained from leaves using comparable and homologated analytical methods (see pages 9-13, ICP forests manual Sampling and Analysis of Needles and Leaves, http://icp-forests.org/manual.htm). The N, P, K, S, Ca and Mg pairwise ratios were calculated on a mass basis. Nutrient concentrations for the same species from different databases were analyzed using mixed models, with database as a fixed factor and country as a random factor. No significant differences were found. All foliar samples had been collected between 1990 and 2015. We only used data from georeferenced plots. **Fig. S1** shows the distribution of the plots.

Data for climate, soil and N and P deposition. Climatic and soil data were added to the foliar stoichiometric data using the *raster* package in R (v. 2.6-7). These data were obtained from the WorldClim 2.0 database[50], with a resolution of 1 km^2 at the equator: minimum average temperature, maximum average temperature, average solar radiation, maximum wind speed, average wind speed, mean water vapor pressure, mean annual temperature (MAT), mean diurnal range, isothermality, temperature seasonality, maximum temperature of the warmest month, minimum temperature of the coldest month, annual temperature range, mean temperature of the wettest quarter, mean temperature of the driest quarter, mean temperature of the coldest quarter, mean annual precipitation (MAP), mean precipitation of the wettest month, mean precipitation of the driest month, mean precipitation seasonality, mean precipitation of the wettest quarter,

mean precipitation of the driest quarter, precipitation of the warmest quarter and precipitation of the coldest quarter. This climatic model was calculated for a long meteorological time series (1970-2000) based on interpolated values of climatic data provided by meteorological stations throughout the territory and adjusted to the observed topography. Five aridity indices were calculated using the climatic data[51-54].

The data for the deposition of atmospheric N and P were obtained from Global Threats to Human Water Security and River Biodiversity[55], with a resolution of 1 km^2 at the equator. Soil taxonomies (order and suborder) were obtained from the USDA Global Soils Region Map (https://www.nrcs.usda.gov/wps/portal/nrcs/detail/soils/use/?cid=nrcs142p2_054013), which provides a resolution of 1 km^2 at the equator.

Phylogenetic and statistical analyses

Phylogenetic signal. We prepared a phylogenetic tree containing the species in our database to test for phylogenetic signals using R statistical software[56]. We thereby obtained a phylogenetic tree containing a selection of species from PhytoPhylo, an available megaphylogeny of vascular plants[57]. We used the *read.tree* and *drop.tip* functions from the R *ape* package[58] to load the PhytoPhylo tree and remove all species that were not in our database.

We used the *phylosig* function from the R *phytools* package[59] to test for phylogenetic signals in the foliar elemental compositions of the species and therefore to determine the extent to which foliar N, P, K, S, Ca and Mg concentrations, pairwise ratios and PCA scores had phylogenetic signals. The *phylosig* function calculates statistics of a phylogenetic signal (Pagel's λ) and *P* values based on the variance of phylogenetically independent contrasts relative to tip shuffling randomization[60]. We chose to analyze the phylogenetic signals in the data using Pagel's λ assumption, based on a study by Münkemüller et al. (2012)[61] comparing the advantages and disadvantages of various methods for estimating phylogenetic signals. Pagel's λ method can provide reliable measurements of effect size and can discriminate between more complex models of trait evolution (such as polygenic organismic traits)[62]. Mean λ in Pagel's method does not change as the number of species in a phylogeny increases and is recommended for large phylogenies with >50 species (or taxa)[63], unlike other methods.

We also used the *contMap* function of the *phytools* package to graphically reconstruct the values of the traits that had a phylogenetic signal across our phylogeny. We used the ape package[50] to load the phylogenetic tree and select the species in it. The *contMap* function estimates the ancestral characters at internal nodes using maximum likelihood and assuming Brownian motion as a model for trait evolution[55] and then interpolates the ancestral condition along the branches of the tree[54]

BN size. "BN size" is another interesting trait when comparing taxa. We thus conducted a functional discriminant analysis (FDA) to determine whether different but closely related species typical of different environments (from more to less climatic stress) tended to have different BN sizes. We compared five of

399 the most important forest species in Europe: *Quercus petraea*, *Q. robur*, *Q. ilex*, *Pinus pinaster* and *P.*
400 *halepensis*. All five species were represented at 600-800 sites in our database across their distributions.
401 FDA is a multivariate analysis that derives the optimal separation between groups (here the different sets of
402 individuals of each species) by maximizing between-group variance and minimizing within-group variance
403 of the set of independent continuous variables used in the analysis (here the foliar N, P, K, S, Ca and Mg
404 concentrations and their pairwise ratios)[65]. We compared the range of scores in the first two roots of the
405 FDA as a measure of the size of the "niche space" of each species. The first two roots of the FDA
406 explained 95.8% of the variance in the foliar elemental composition of the various species. We then
407 analyzed the roles of phylogeny and species in the dispersion of the canonical scores on the root axes of the
408 FDA using Bayesian phylogenetic linear mixed models and the MCMCglmm package[66] in R. Phylogeny
409 and species were included as random factors: the phylogenetic term accounted for variability in the shared
410 ancestry, and the species term accounted for species-specific traits independent of the shared ancestry.
411
412 Analysis of the relationships of foliar elemental composition with climatic variables and N deposition. We
413 tested the effects of climate and N deposition on the foliar concentrations of the bioelements, their ratios
414 and PC scores (of the PCA of all elemental foliar concentrations and their pair-wise ratios) using Bayesian
415 phylogenetic linear mixed models and the MCMCglmm package[66] in R. We used MAT, MAP, annual
416 radiation, mean annual vapor pressure deficit VPD, range of diurnal temperatures and N deposition as fixed
417 effects. Phylogeny and species were included as random factors: the phylogenetic term accounted for the
418 variability in the shared ancestry, and the species term accounted for species-specific traits independent of
419 the shared ancestry. Both random factors together thus accounted for the variance explained by heritability.
420 We repeated these analyses using soil type instead of climate and N deposition as fixed effects.
421
422 Analysis of the relationships between foliar elemental composition and soil type. We analysed the
423 differences of the foliar variables among the various soil types (taxonomic orders). A soil map was
424 generated using the R *raster* and *rgdal* packages to obtain the soil classifications for each sample location.
425 We chose soil type (orders of soil taxonomy) as the most accurate taxon at the pixel scale in the USDA
426 Global Soils Region Map. No data were found for Gelisols or Aridisols. We tested the effect of soil
427 order on the foliar concentration of bioelements, their ratios and PC scores (of the PCA of all elemental
428 foliar concentrations and their pair-wise ratios) using Bayesian phylogenetic linear mixed models and the
429 MCMCglmm package[66] in R. We used soil orders as fixed effects. Phylogeny and species were included as
430 random factors: the phylogenetic and species terms were introduced as random factors accounting for the
431 variance explained by heritability, as described previously.
432 We performed PCAs of foliar N, P, K, Ca, Mg and S concentrations and N:P ratios to further explore the
433 relationships between trees growing under different soil types and their overall elemental compositions. We
434 then analyzed the scores of the PC1 and PC2 axes to detect differences in overall foliar elemental

composition depending on the order of the soil in which they grew using Bayesian phylogenetic linear mixed models and the MCMCglmm package[66] in R, in which the first three PCA axes were the response variables and soil order was the fixed predictor. Phylogeny and species were included as random factors, as in the previous analysis of the FDA scores. Model parameters (soil types) with non-overlapping 95% credible intervals were considered to differ significantly.

Analysis of differences in species foliar elemental composition and stoichiometry between populations growing in different communities with different species compositions. We used the map of species distribution in the European Information System on Forest Genetic (EUFGIS) database http://portal.eufgis.org/data/. We compared the foliar N, P and K concentrations of pairwise species with comparable co-occurring and non-co-occurring surfaces with an overlapping distribution between 25 and 75%. We established sets of individuals in the overlapping area between the compared species and both areas where only one of the species was present. The data were analyzed in R using the packages raster (v. 3.4.3), rgeos (v. 3.4.4), maptools (v. 3.4.3), maps (v. 3.4.3), rworldmap (v. 3.4.4), ggmap (v. 3.4.3) and rworldxtra (v. 3.4.4). We used these tools to choose species with large distributions and many datapoints in our database (600-800) and combined species in several possible pairs. We compared the two portions of the global distributions for each species of each pair that overlapped or not with the distribution of the other species. An ANOVA compared the N, P and K concentrations and PC1 and PC2 scores (from the PCA of the six bio-elements and their pairwise ratios) for each species inside and outside the overlapping zone (with or without competition between the two species, respectively).

Acknowledgements

The authors would like to acknowledge the financial support from the European Research Council Synergy grant ERC-SyG-2013-610028 IMBALANCE-P, the Spanish Government grant PID2019-110521GB-I00 and the Catalan Government grant SGR 2017-1005. M.F.-M. is a postdoctoral fellow of the Research Foundation – Flanders (FWO).

References

1.Tracy, C.R. &Christian, K.A. Ecological relations among space, time, and thermal niche axes. *Ecology*, **67**, 609-615 (1986).
2.Peterson, A. T., Soberon, J.& Sanchez-Cordero, V, Conservatism of ecological niches in evolutionary time. *Science* **285**, 1265-1267 (1999).
3.Hirzel, A. H,., Hausser, J., Chessel, D. & Perrin, N. Ecological-niche factor analysis: How to compute habitat-suitability maps without absence data? *Ecology* **83**, 2017-2036 (2002).
4.Sexton, J. P., Montiel, J., Shay, J. E., Stephens, M. R. & Slatyer, R. A. Evolution of ecological niche breadth. *An. Rev. Ecol. Evol. Syst.* **48**, 183-206 (2017).
5.Wright, J. W., Davies, K. F., Lau, J. A., McCall, A. C. & McKay, J. K. Experimental verification of ecological niche modelling in a heterogeneous environment. *Ecology* **87**, 2433-2439 (2006).
6. Swanson, H. K. et al. A new probabilistic method for quantifying n-dimensional ecological niches and niche overlap. *Ecology* **96**, 318-324 (2015).
7.Grubb, P. J. The maintenance of species-richness in plant communities: the importance of the regeneration niche. 1977. *Biol. Rev*. **52**, 107-145 (1977).
8.Herrel, A., Spithoven, L., Van Damme, V. & De Vree F. Sexual dimorphism of head size in *Gallotia galloti*: testing the divergence hypothesis by functional analyses. *Funct. Ecol.* **13**, 289-297 (1999).

9.Mouillot, D. et al. Niche overlap estimates based on quantitative functional traits: a new family of non-parametric indices. *Oecologia* **145**, 345-353 (2005).
10.Kraft, N., Valencia, R. & Ackerly D.D. Functional traits and niche based tree community assembly in an amazonian forest. *Science* **322**, 580-582 (2008).
11.Peñuelas, J., Sardans, J., Ogaya, R.,& Estiarte, M. Nutrient stoichiometric relations and biogeochemical niche in coexisting plant species: effect of simulated climate change. *Pol. J. Ecol.* **56**, 613-622 (2008).
12.Peñuelas J. et al. Faster returns on "leaf economics" and different biogeochemical niche in invasive compared with native plant species. *Glob. Change Biol*. **16**, 2171-2185 (2010).
13.Peñuelas, J. et al. The bioelements, the elementome and the "biogeochemical niche". *Ecology* **100**, e02652 (2019).
14.Sardans, J. et al.Factors influencing the foliar elemental composition and stoichiometry in forest trees in Spain. *Persp. Plant Ecol. Evol. Syst*. **18**, 52–69 (2016).
15.Sardans, J. et al. Foliar elemental composition of European forest tree species associated with evolutionary traits and present environmental and competitive conditions. *Glob. Ecol. Biogeogr*. **24**, 240-255 (2015).
16.Urbina, I.et al. Shifts in the elemental composition of plants during a very severe drought.*Environ.Exp. Bot*. **111**, 63-73 (2015).
17.Urbina, I. et al. Plant community composition affects the species biogeochemical niche. *Ecosphere* **8**, e01801 (2017).
18. White, P.J. et al. Testing distinctness of shoot ionomes of angiosperm families using the Rothamsted Park grass continuous hay experiment. *New Phytologist* **196**, 101-109 (2012).
19.Kerkhoff, A. J., Fagan, W. F., Elser, J. J., Enquist, B. J. Phylogenetic and growth form variation in the scaling of nitrogen and phosphorus in the seed plants. *The Am. Nat.168*, E103-E122 (2006).
20. Sardans, J. Janssens, I. A., Ciais P., Obersteiner, M., Peñuelas J. Recent advances, approaches and future research in ecological stoichiometry: towards a novel holistic theory in ecology. Biogeochemistry. Submitted.
21. Neugebauer, K. et al. Variation in the Angiosperm Ionome. *Physiol. Plant*. **163**, 306-322 (2018).
22.Gillman, L. N., Keeling, D. J., Gardner, R.C. & Wright, S.D. Faster evolution of highly conserved in tropical plants. *J. Evol. Biol*. **23**, 1327-1330 (2010).
23.Puurtinen, M. et al. Temperature-dependent mutational robustness can explain faster molecular evolution at warm temperatires, affecting speciation rate and global patterns of species diversity. *Ecography* **39**, 1025-1033 (2016).
24.Kellner, A., Ritz, C. M., Schlittenhaedt, P. & Hellwig, F. H. Genetic differentiation in the genus Lithps L. (Ruschoideae, Aizoaceae) revelas a high level of convergent evolution and reflects geographic distribution. *Plant Biol*. **13**, 368-380 (2011).
25.Jwa, N. S. & Hwang, B. K. Convergent evolution of pathogen effectors toward reactive oxygen species signaling networks in plants. *Front. Plant Sci*. **8**, 1687 (2017).
26.Molina-Montenegro, M.A et al. Is the causes of plant invasions the result of rapid adaptive evolution in seed traits? evidence a latitudinal rainfall gradient? *Front. Plant Sci*. **9**, 208 (2018).
27.Anacker, B. L. & Strauss, S. Y. Ecological similarity is related to phylogenetic distance between species in a cross-niche field transplant experiment. *Ecology* **97**, 1807-1818 (2016).
28.Reich, P. B. & Oleksyn, J. Global patterns of plant leaf N andP in relation to temperature and latitude. *Proc. Natl. Acad.Sci. USA* **101**, 11001–11106 (2004).
29.Ordoñez, J. C. et al. A global study of relationshipsbetween leaf traits, climate and soil measures of nutrientfertility. *Glob. Ecol. Biogeogr*. **18**, 137–149 (2009).
30.Kerkhoff, A. J., Enquist, B. J., Elser, J. J. & Fagan, W. F. Plantallometry, stoichiometry and the temperature-dependenceof primary productivity. *Glob. Ecol. Biogeogr*. **14**, 585–598 (2005).
31.Yuan Z. Y. & Chen, H. Y. H. Global trends in senesced-leafnitrogen and phosphorus. *Glob. Ecol. Biogeogr*.**18**, 532–542 (2009).
32.Vitousek, P. M., Porder, S., Houlton, B. Z. & Chadwick, O. A. Terrestrial phosphorus limitation: mechanisms, implications and nitrogen-phosphorus interactions. *Ecol. Appl*. **20**, 5–15 (2010).
33.McGroddy, M. E., Daufresne, T. & Hedin, L. O. Scaling of C/N/P stoichiometry in forest worldwide: implications ofterrestrial Redfield-type ratios. *Ecology* **85**, 2390–2401 (2004).
34.Townsend, A. R., Cleveland, C. C., Asner, G. P. & Bustamante, M. M. C. Controls over foliar N:P ratios in tropical rainforest. *Ecology* **88**, 107–118 (2007).
35.Lovelock, C. E., Feller, I. C., Ball, M. C., Ellis, J. & Sorell, B. Testing the growth rate vs. geochemical hypothesis for latitudinal variation in plant nutrients. *Ecol. Lett*. **10**, 1154–1163 (2007).
36.Marschner, H. *Mineral nutrition of higher plants*, London. Academic Press (1995).
37.Zhang, Y., Mathur, R., Bash, J. O., Hogrefe, C., Xing, J. & Roselle, S. J. Log-term trends in total inorganic nitrogen and sulfur deposition in US from 1990 to 2010. *Atm. Chem. Phys*. **18**, 9091-9106 (2018).
38.Horn, K, J. et al. Growth and survival relationships of 71 tree species with nitrogen and sulfur deposition across the conterminous U.S. *PlosOne* **14**, e0212984 (2019).

39.Papanikolaou, N., Britton, A. J., Helliwell, R. C. & Johnson, D. Nitrogen deposition, vegetation burning and climate warming act independently on microbial community structure and enzyme activity associated with decomposing litter in low-alpine heath. *Glob. Change Biol*. **16**, 3120–3132 (2010).
40.Marklein, A. R. & Houlton, B. Z. Nitrogen inputs accelerate phosphorus cycling rates across a wide variety of terrestrial ecosystems. *New Phytol*. **193**, 696–704 (2012).
41Sardans, J. et al. Foliar and soil concentrations and stoichiometry of nitrogen and phosphorous across European *Pinus sylvestris* forests: relationships with climate, N deposition and tree growth. *Funct. Ecol*. **30**, 676-689 (2016).
42.Peñuelas J. et al. Human-induced nitrogen-phosphorus imbalances alter natural and managed ecosystems across the globe. *Nature Com.* **4**, 2934 (2013).
43.Peñuelas, J. et al. Increasing atmospheric CO_2 concentrations correlate with declining nutritional status of European forests. *Com. Biol*. **3**, 125 (2020).
44.Ahmad, N. & Mermut, A. Vertisols and Tachnologies for their Management. Development in Soil Science 24. Elsevier. Amsterdam. 302 pp (1996).
45.Nishiue, A., Nanzyo, M., Kanno, H.& Takahashi, T. Properties and classification of volcanic ash soils around Lake Kuwanuma on the eastern footslope of Mt. Funagata in Miyagi prefecture, northeastern Japan. *Soil Sci. Plant Nutr*. **60**, 848-862 (2014).
46. de la Riva, E. G. et al. Biogeochemical and Ecomorphological Niche Segregation of Mediterranean Woody Species along a Local Gradient. *Fron. Plant Sci.* **8**, 1242 (2017).
47.Yu, Q. et al. Stoichiometry homeostasis of vascular plants in the inner Mongolia grassland. *Oecologia* **166**, 1–10 (2011).
48.Sardans, J., Albert Rivas-Ubach, A. & Peñuelas, J. The elemental stoichiometry of aquatic and terrestrial ecosystems and its relationships with organismic lifestyle and ecosystem structure and function: a review. *Biogeochemistry* **111**, 1–39 (2012).
49.Gracia, C., Burriel, J. A., Ibàñez, J. J., Mata, T. & Vayreda, J. *Inventari ecològic i forestal de Catalunya. Mètodes*, Vol. 9. CREAF, Bellaterra (2004).
50.Fick, A. E. & Hijmans, R. J. WorldClim 2: new 1-km spatial resolution climate surfaces for global land areas. *Int. J. Climatol*. **37**, 4302-4315 (2017).
51.Lang, R. Verwitterung und Bodenbildung als Einfuehrung in die Bodenkunde. Schweizerbart Science Publishers, Stuttgart (1920).
52.Köppen, W. Klassification der Klimate nach Tempertur, Niederschlag and Jahreslauf. *Petermanns Geog. Mitt.* **64**, 243–248 (1918).41.De Martonne, E. Aréisme et Indice d'Aridité. *Comptes Rendus Acad. Sci.* **181**, 1395-1398 (1926).
53.De Martonne, E. Nouvelle carte mondiale de l'indece d'aridité. Annales de Géographie 51, 242-250 (1942).
54.Emberger, L. La vegetation de la región mèditerranéenne, essai d'une classification des groupements vegetaux. *Rev. Gén. Bot*. **648** (1930).
55.Vorösmarty, C. J. et al. Global threats to human water security and river biodiversity. *Nature* **467**, 555-561 (2010).
56.R Development Core Team. *R: a language and environment for statistical computing*. R Foundation for StatisticalComputing, Vienna. Available at: http://www.R-project.org/. (2011).
57. Qian, H., Jin, Y. An updated megaphylogeny of plants, a tool for generating plant phylogenies, and an analysis of phylogenetic community structure. *J. Plant Ecol*. **9**, 233–239 (2016).
58.Paradis, E., Claude, J. & Strimmer, K. (2004) APE: analyses o fphylogenetics and evolution in R language. *Bioinformatics* **20**, 289–290 (1999).
59.Revell, L. J. Phytools: An R package for phylogenetic comparative biology (and other things). *Methods Ecol. Evol.* **3**, 217–223 (2012).
60. Blomberg, S.P., Garland, T., Ives, A.R. Testing for phylogenetic signal in comparative data: behavioral traits are more labile. *Evolution* **57**, 717–45 (2003).
61.Münkemüller, T. et al. How to measure and test phylogenetic signal. *Methods Ecol. Evol*. **3**, 743-756 (2012).
62.Pagel, M. Inferring the historical patterns of biological evolution. *Nature* **401**, 877–884 (1999).
63.Felsenstein, J. Phylogenies and the comparative method. *Am. Nat.* **125**, 1–15 (1985).
64.Revell, L. J. Two new graphical methods for mapping trait evolution on phylogenies. *Methods Ecol. Evol*. **4**, 754–759 (2013).
65.Ramos, S. D. S. & Liow, S. R. . Discriminant Functional Analysis. Ed: Chapelle, C.A. The Encyclopedia of Applied Linguistics, Chapter: Discriminant Function Analysis, Publisher: John Wiley & Sons (2012), Ed: Chapelle, C.A.66. Hadfield, J. D. MCMC methods for multi-response generalised linear mixed models: the MCMCglmm R package. *J. Stat. Softw.* **33**, 1–22 (2010).

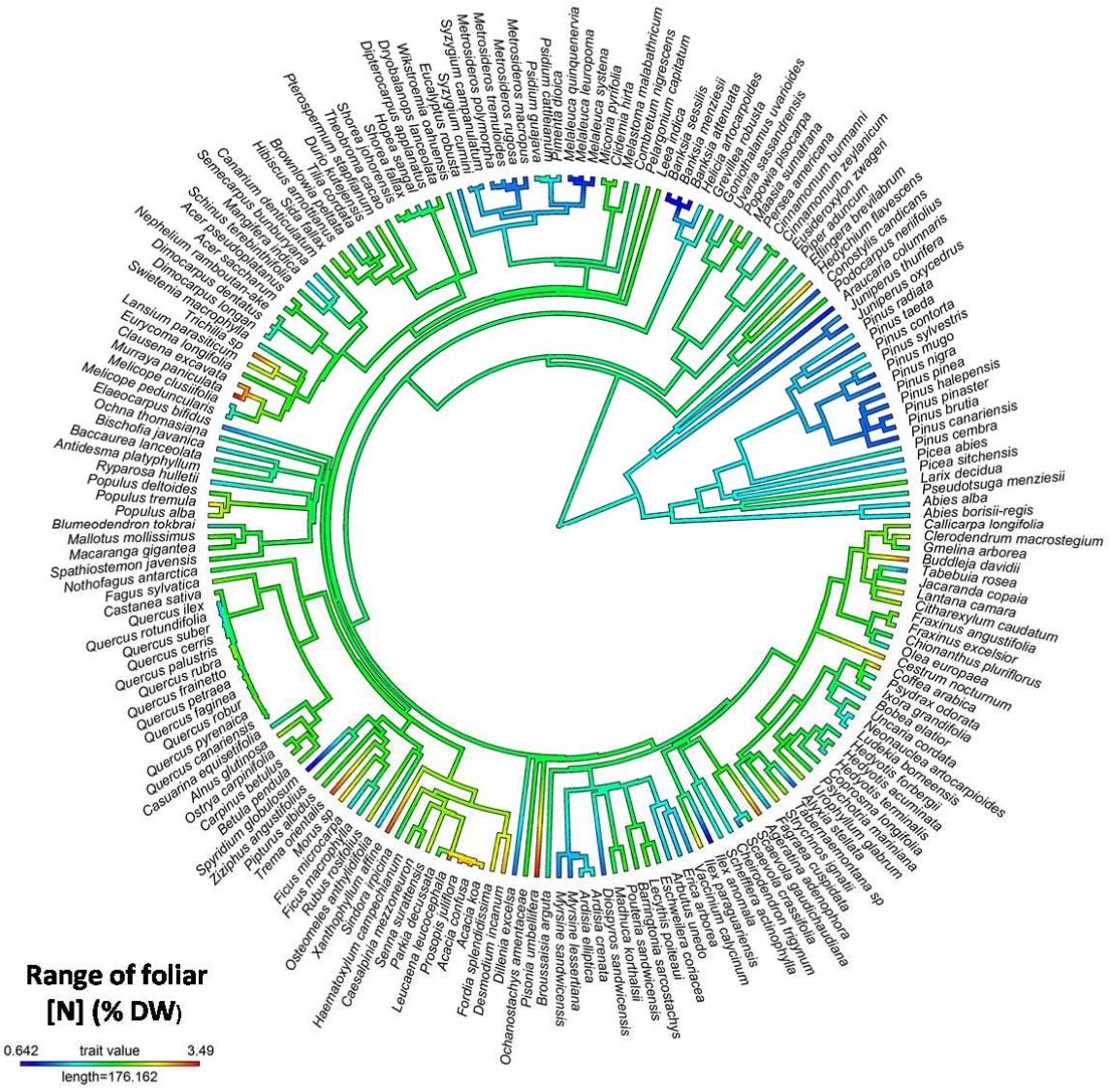

Fig. 1. Phylogenetic diagrams of the foliar N concentration in the phylogenetic tree obtained using the *contMap* function of the *phytools* package in R, representing the value structure used to estimate the phylogenetic signals in the variables. The *contMap* function estimates the ancestral characters at internal nodes using maximum likelihood and assuming Brownian motion as a model for trait evolution[61] and then interpolates the ancestral condition along the branches of the tree[62]. DW Dry weight.

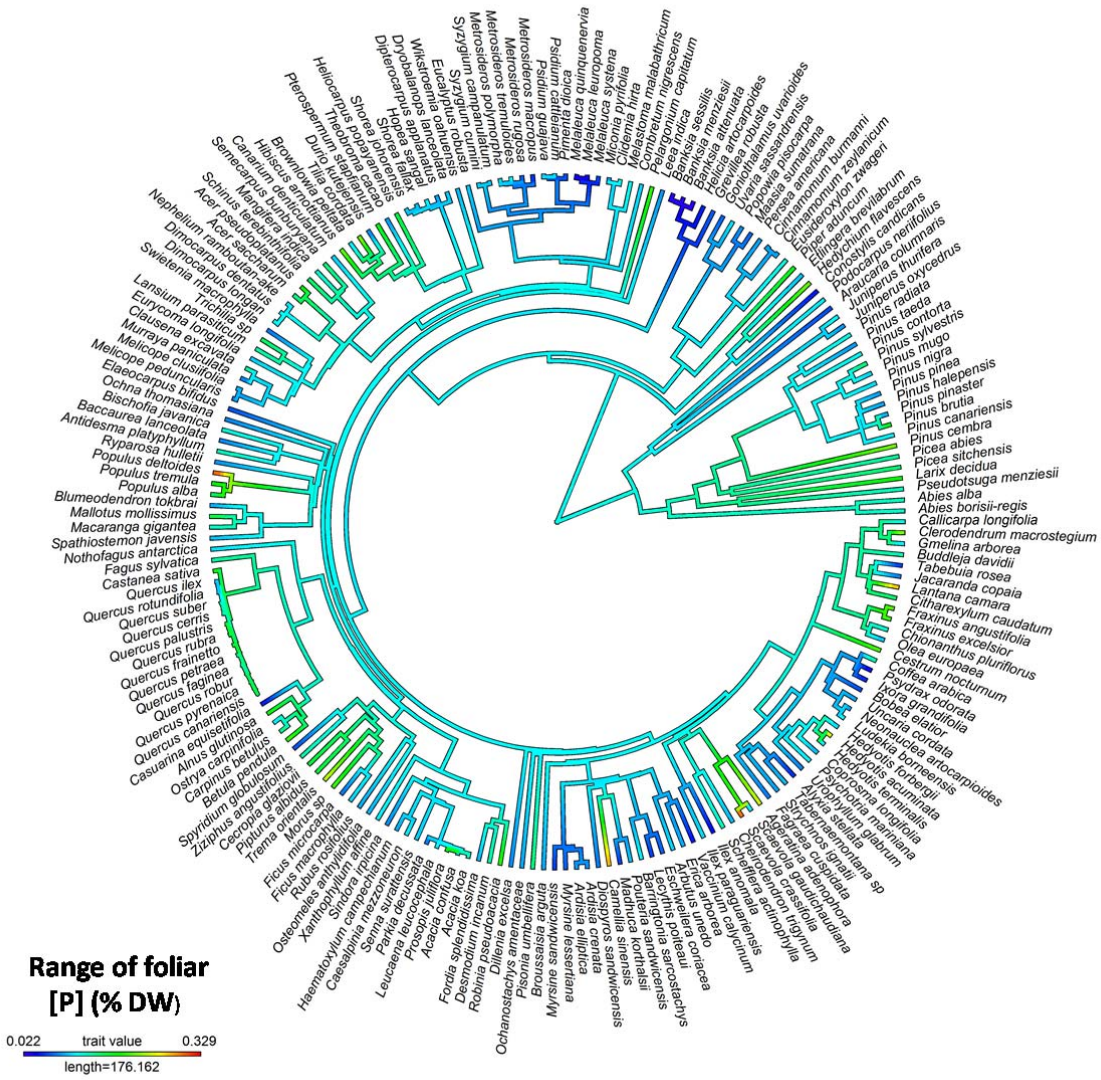

609
610
611
612 **Fig. 2.** Phylogenetic diagrams of the foliar P concentration in the phylogenetic tree obtained using the *contMap* function of the
613 *phytools* package in R, representing the value structure used to estimate the phylogenetic signals in the variables. The *contMap*
614 function estimates the ancestral characters at internal nodes using maximum likelihood and assuming Brownian motion as a model
615 for trait evolution[61] and then interpolates the ancestral condition along the branches of the tree[62]. DW Dry weight
616
617
618
619
620
621
622
623
624
625

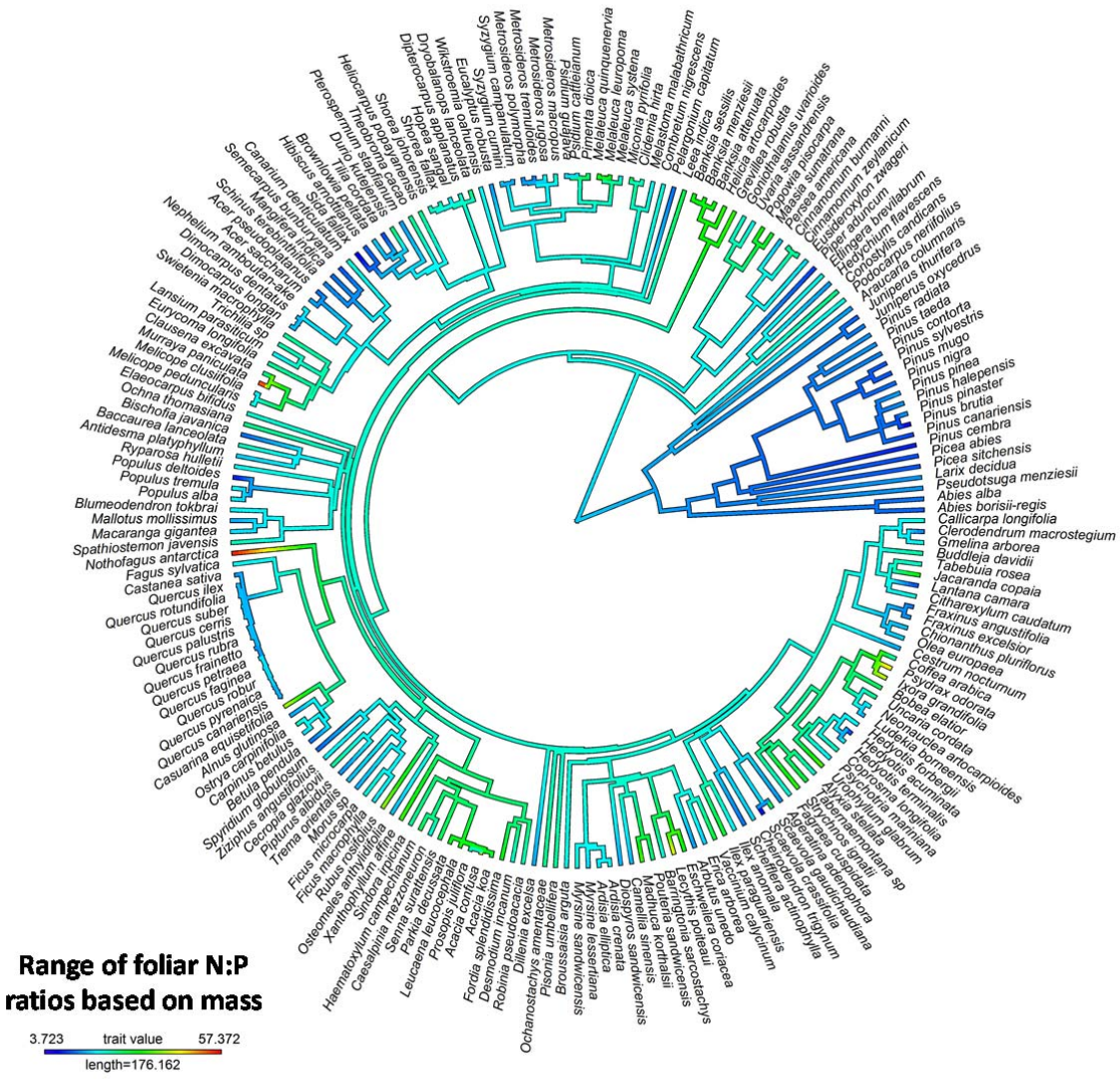

Fig. 3. Phylogenetic diagrams of the foliar N:P ratio in the phylogenetic tree obtained using the *contMap* function of the *phytools* package in R, representing the value structure used to estimate the phylogenetic signals in the variables. The *contMap* function estimates the ancestral characters at internal nodes using maximum likelihood and assuming Brownian motion as a model for trait evolution[61] and then interpolates the ancestral condition along the branches of the tree[62].

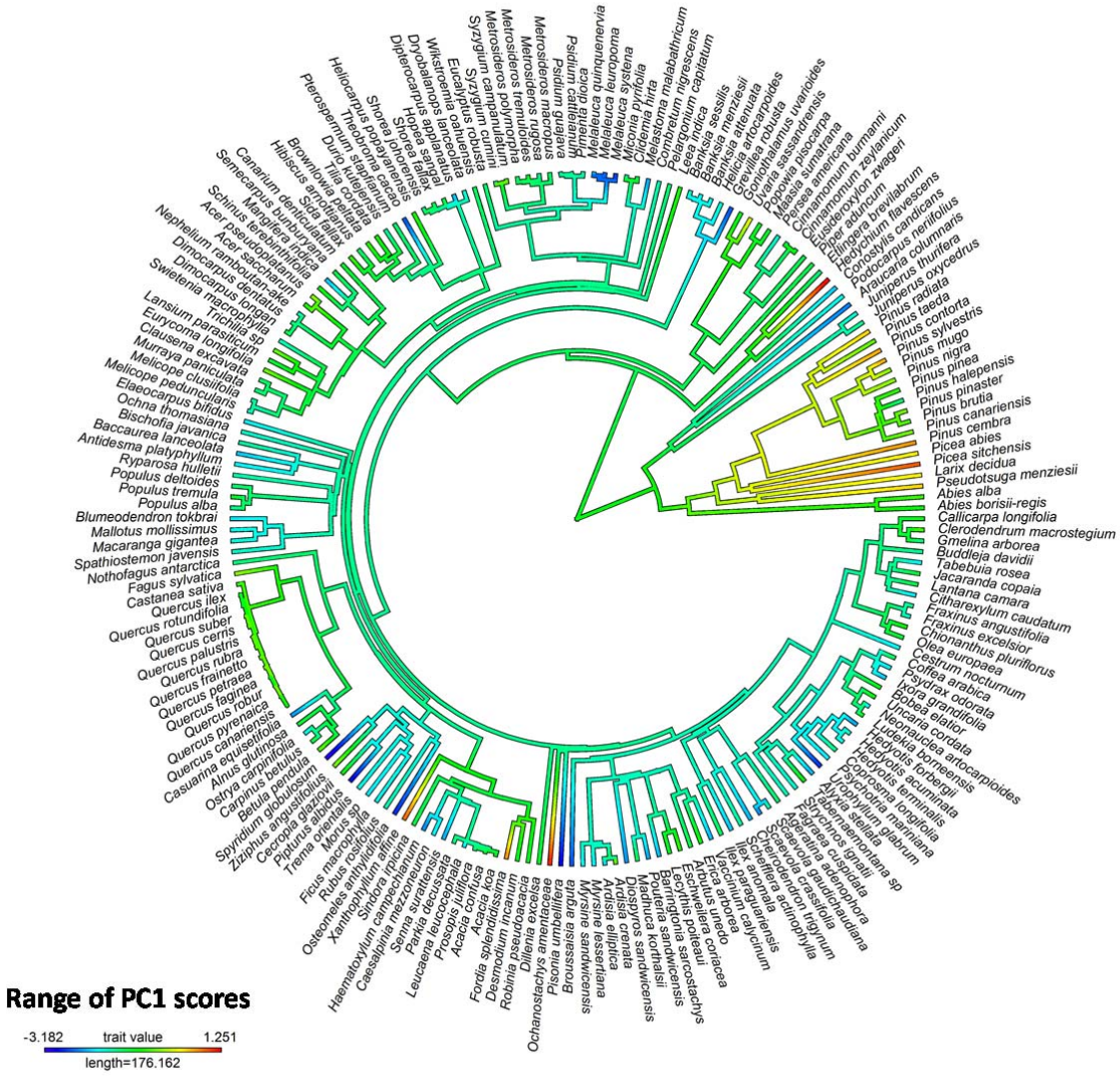

Fig. 4. Phylogenetic diagrams of the PC1 scores in the phylogenetic tree obtained using the *contMap* function of the *phytools* package in R, representing the value structure used to estimate the phylogenetic signals in the variables. The *contMap* function estimates the ancestral characters at internal nodes using maximum likelihood and assuming Brownian motion as a model for trait evolution[61] and then interpolates the ancestral condition along the branches of the tree[62].

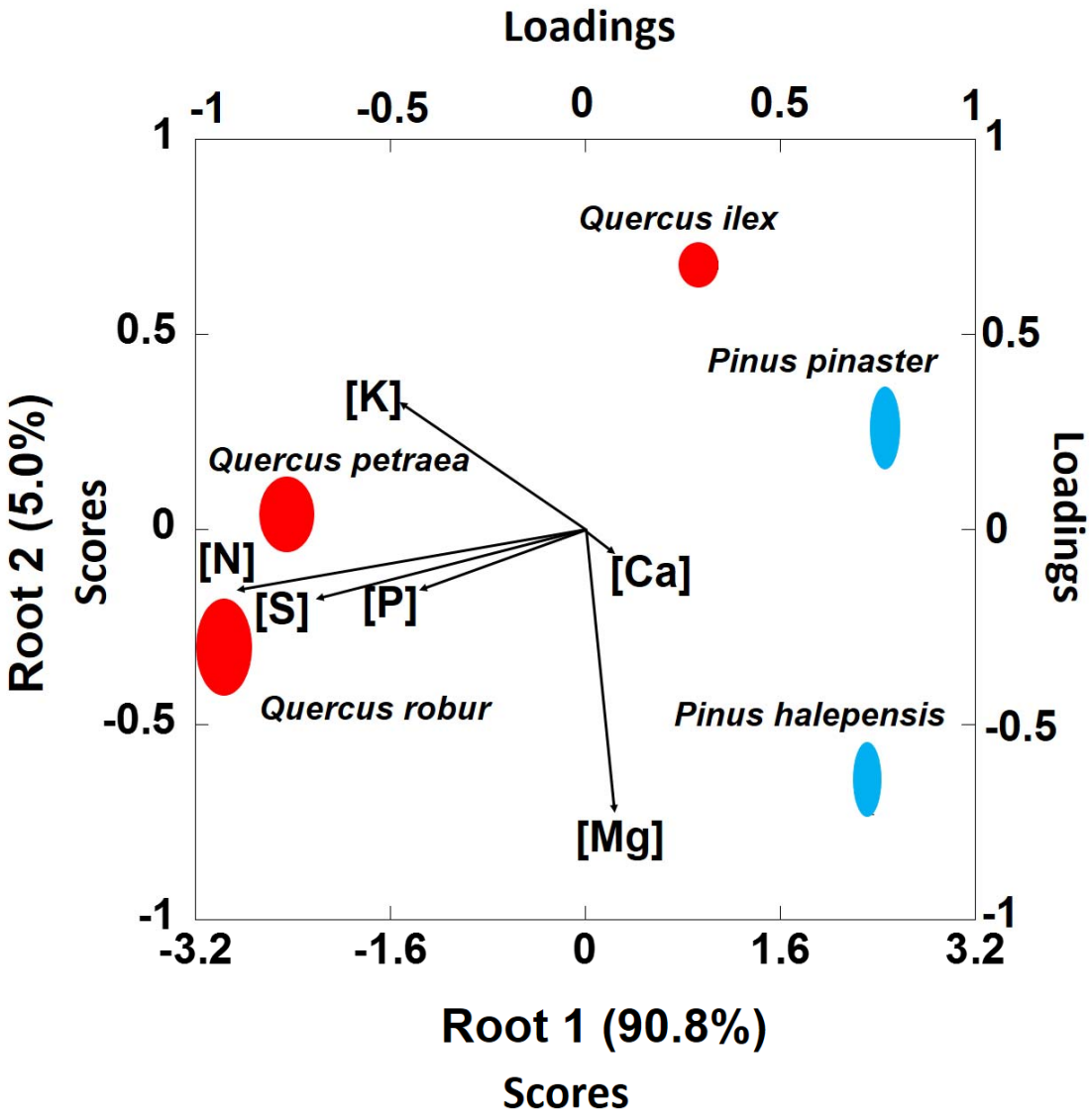

Fig. 5. Plot of the first two roots of the functional discriminant analysis using *Pinus pinaster*, *P. halepensis*, *Quercus ilex*, *Q. petraea* and *Q. robur* as dependent categorical grouping factors and foliar N, P, K, S, Ca and Mg concentrations and pairwise ratios as continuous independent variables. The plot depicts the 95% confidence interval of the mean corresponding to each species and the variable loadings on Roots 1 and 2.

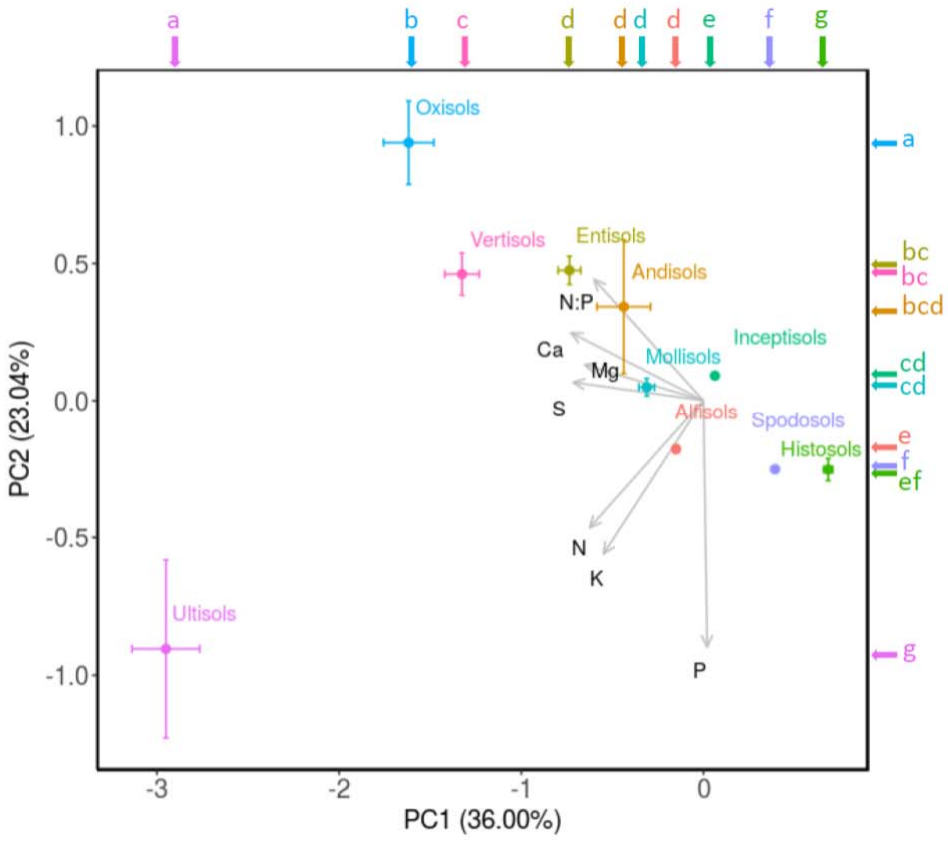

Fig. 6. Plot of the PCA cases and variables superimposed, defined by the first two components of the PCA, with foliar N, P, K, Ca, Mg and S concentrations as variables and with soil orders as cases. Different letters on the arrows at the right indicate significant differences (P<0.05). Error bars indicate the 95% confidence intervals.

674
675
676
677
678
679
680
681
682

683
684
685
686
687
688
689
690

691
692

693

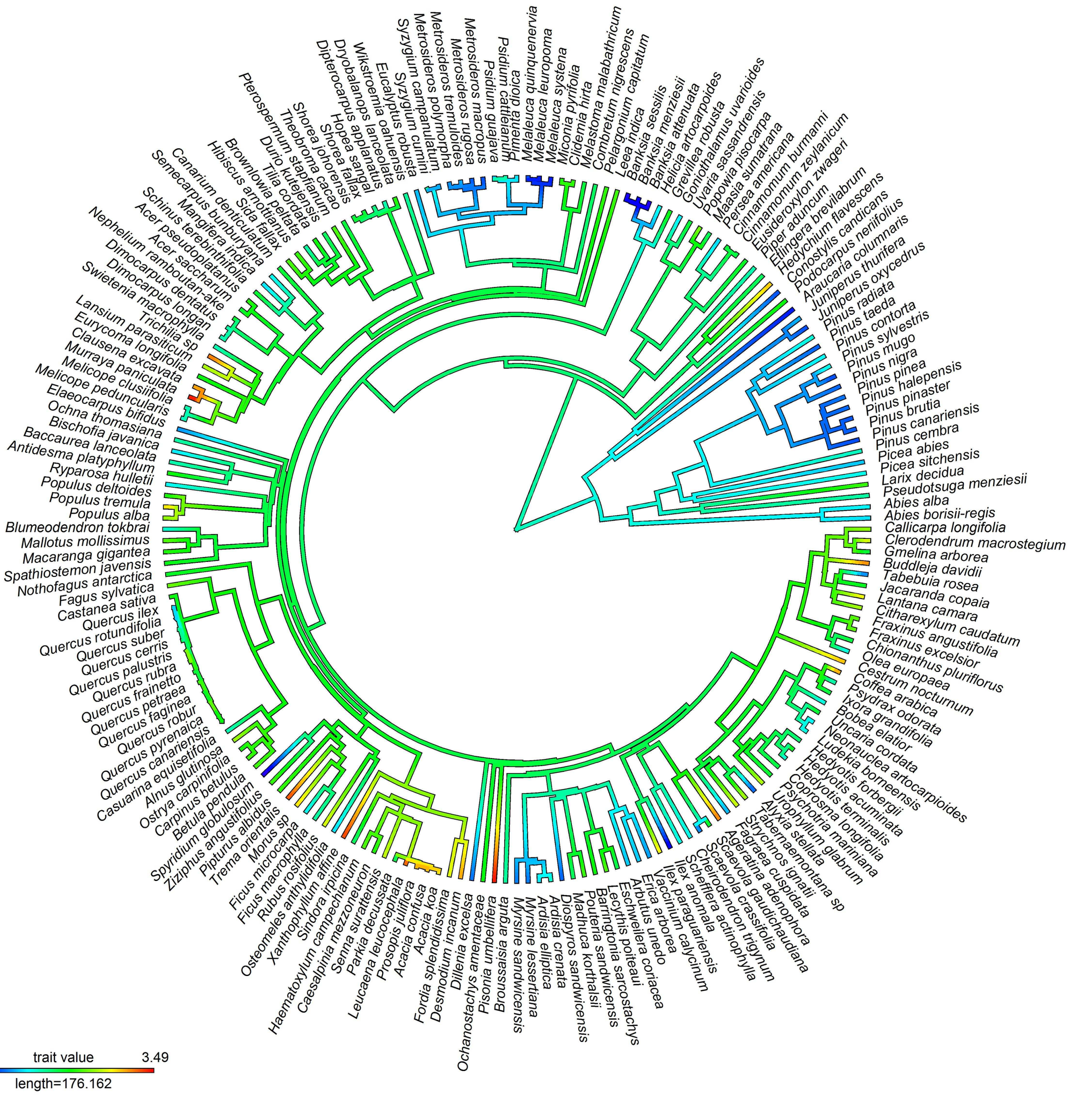
Psidium cattleianum
Psidium guajava
Pimenta dioica
Melaleuca quinquenervia
Melaleuca leuropoma
Melaleuca systena
Miconia pyrifolia
Clidemia hirta
Melastoma malabathricum
Combretum nigrescens
Pelargonium capitatum
Leea indica
Banksia sessilis
Banksia menziesii
Banksia attenuata
Helicia artocarpoides
Grevillea robusta
Goniothalamus uvarioides
Uvaria sassandrensis
Popowia pisocarpa
Maasia sumatrana
Persea americana
Cinnamomum burmanni
Cinnamomum zeylanicum
Cinnamomum zwageri
Euusideroxylon zwageri
Piper aduncum
Eitingera brevilabrum
Hedychium flavescens
Conostylis candicans
Podocarpus neriifolius
Araucaria columnaris
Juniperus thurifera
Juniperus oxycedrus
Pinus radiata
Pinus taeda
Pinus contorta
Pinus sylvestris
Pinus mugo
Pinus nigra
Pinus pinea
Pinus halepensis
Pinus pinaster
Pinus brutia
Pinus canariensis
Pinus cembra
Picea abies
Picea sitchensis
Larix decidua
Pseudotsuga menziesii
Abies alba
Abies borisii-regis
Callicarpa longifolia
Clerodendrum macrostegium
Gmelina arborea
Buddleja davidii
Tabebuia rosea
Jacaranda copaia
Lantana camara
Citharexylum caudatum
Fraxinus angustifolia
Fraxinus excelsior
Chionanthus pluriflorus
Olea europaea
Cestrum nocturnum
Coffea arabica
Psydrax odorata
Ixora grandifolia
Bobea elatior
Uncaria cordata
Neonauclea artocarpioides
Ludekia borneensis
Hedyotis terminalis
Hedyotis forbergii
Hedyotis longifolia
Coprosma marriniana
Psychotria glabrum
Urophyllum stellata
Alyxia stellata
Tabernaemontana sp
Strychnos ignatii
Fagraea cuspidata
Ageratina adenophora
Scaevola gaudichaudiana
Scaevola crassifolia
Cheirodendron trigynum
Schefflera actinophylla
Ilex anomala
Ilex paraguariensis
Vaccinium calycinum
Erica arborea
Arbutus unedo
Eschweilera coriacea
Lecythis poiteaui
Barringtonia sarcostachys
Pouteria sandwicensis
Madhuca korthalsii
Diospyros sandwicensis
Myrsine sandwicensis
Myrsine lessertiana
Ardisia elliptica
Ardisia crenata
Broussaisia arguta
Pisonia umbellifera
Ochanostachys amentaceae
Dillenia excelsa
Desmodium incanum
Fordia splendidissima
Acacia koa
Acacia confusa
Prosopis juliflora
Leucaena leucocephala
Parkia decussata
Senna surattensis
Caesalpinia mezzoneuron
Sindora irpicina
Haematoxylum campechianum
Xanthophyllum affine
Osteomeles anthyllidifolia
Rubus rosifolius
Ficus macrophylla
Ficus microcarpa
Morus sp
Trema orientalis
Pipturus albidus
Ziziphus angustifolius
Spyridium globulosum
Betula pendula
Carpinus betulus
Ostrya carpinifolia
Alnus glutinosa
Casuarina equisetifolia
Quercus canariensis
Quercus pyrenaica
Quercus robur
Quercus faginea
Quercus petraea
Quercus frainetto
Quercus rubra
Quercus palustris
Quercus cerris
Quercus suber
Quercus rotundifolia
Quercus ilex
Castanea sativa
Fagus sylvatica
Nothofagus antarctica
Spathiostemon javensis
Macaranga gigantea
Mallotus mollissimus
Blumeodendron tokbrai
Populus alba
Populus tremula
Populus deltoides
Ryparosa hulletii
Antidesma platyphyllum
Baccaurea lanceolata
Bischofia javanica
Ochna thomasiana
Elaeocarpus bifidus
Melicope peduncularis
Melicope clusiifolia
Murraya paniculata
Clausena excavata
Eurycoma longifolia
Lansium parasiticum
Trichilia sp
Swietenia macrophylla
Dimocarpus longan
Dimocarpus dentatus
Nephelium ramboutan-ake
Acer pseudoplatanus
Acer saccharum
Schinus terebinthifolia
Mangifera indica
Semecarpus bunburyana
Canarium denticulatum
Hibiscus arnottianus
Sida fallax
Brownlowia peltata
Tilia cordata
Durio kutejensis
Pterospermum stapfianum
Theobroma cacao
Shorea johorensis
Hopea fallax
Shorea sangal
Dipterocarpus applanatus
Dryobalanops lanceolata
Wikstroemia oahuensis
Eucalyptus robusta
Syzygium cumini
Syzygium campanulatum
Metrosideros polymorpha
Metrosideros tremuloides
Metrosideros rugosa
Metrosideros macropus
0.642
trait value
3.49
length=176.162

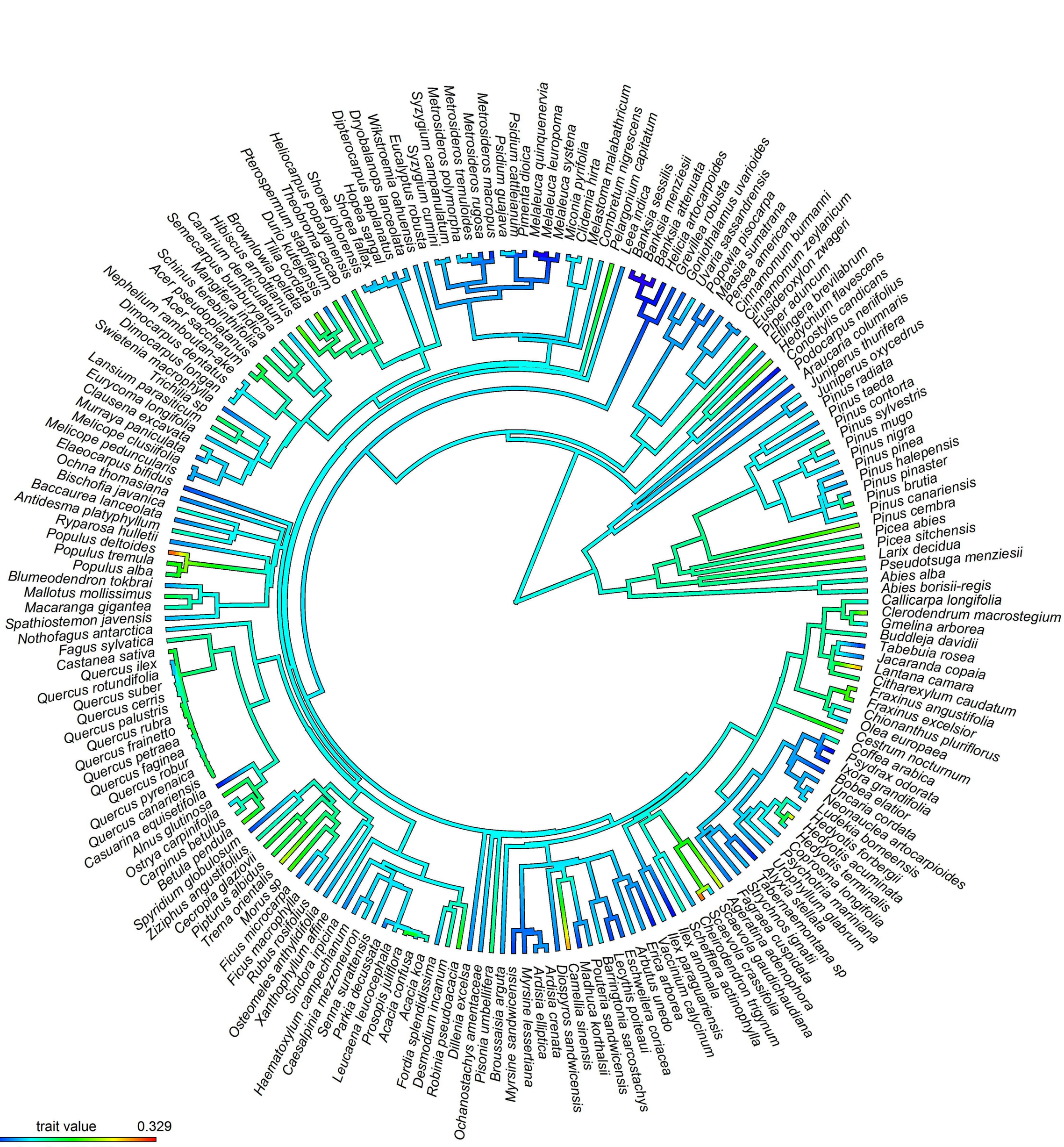
Psidium cattleianum
Psidium guajava
Metrosideros macropus
Metrosideros rugosa
Metrosideros tremuloides
Metrosideros polymorpha
Syzygium campanulatum
Syzygium cumini
Syzygium robusta
Eucalyptus oahuensis
Wikstroemia lanceolata
Dryobalanops applanatus
Dipterocarpus hasseltii
Hopea sangal
Shorea johorensis
Shorea parvifolia
Theobroma cacao
Heliocarpus popayanensis
Pterospermum stapfianum
Durio kutejensis
Tilia cordata
Brownlowia peltata
Hibiscus arnottianus
Canarium denticulatum
Mangifera indica
Semecarpus bunburyana
Schinus terebinthifolia
Acer pseudoplatanus
Acer saccharum
Nephelium ramboutan-ake
Dimocarpus dentatus
Dimocarpus longan
Swietenia macrophylla
Trichilia sp
Lansium parasiticum
Eurycoma longifolia
Clausena excavata
Murraya paniculata
Melicope clusiifolia
Melicope pedunculata
Elaeocarpus bifidus
Ochna thomasiana
Bischofia javanica
Baccaurea lanceolata
Antidesma platyphyllum
Ryparosa hulletii
Populus deltoides
Populus tremula
Populus alba
Blumeodendron tokbrai
Mallotus mollissimus
Macaranga gigantea
Spathiostemon javensis
Nothofagus antarctica
Fagus sylvatica
Castanea sativa
Quercus ilex
Quercus rotundifolia
Quercus suber
Quercus cerris
Quercus palustris
Quercus rubra
Quercus frainetto
Quercus petraea
Quercus faginea
Quercus robur
Quercus pyrenaica
Quercus canariensis
Casuarina equisetifolia
Alnus glutinosa
Ostrya carpinifolia
Carpinus betulus
Betula pendula
Spyridium globulosum
Ziziphus angustifolius
Cecropia glaziovii
Pipturus albidus
Trema orientalis
Morus sp
Ficus microcarpa
Ficus macrophylla
Rubus rosifolius
Osteomeles anthyllidifolia
Xanthophyllum affine
Sindora irpicina
Haematoxylum campechianum
Caesalpinia mezzoneuron
Senna surattensis
Parkia decussata
Leucaena leucocephala
Prosopis juliflora
Acacia confusa
Acacia koa
Fordia splendidissima
Desmodium incanum
Robinia pseudoacacia
Dillenia excelsa
Ochanostachys amentaceae
Pisonia umbellifera
Broussaisia arguta
Myrsine sandwicensis
Myrsine lessertiana
Ardisia elliptica
Ardisia crenata
Diospyros sandwicensis
Camellia sinensis
Madhuca korthalsii
Pouteria sandwicensis
Barringtonia sarcostachys
Lecythis poiteaui
Eschweilera coriacea
Arbutus unedo
Erica arborea
Vaccinium calycinum
Ilex paraguariensis
Ilex anomala
Scheffflera actinophylla
Cheirodendron trigynum
Scaevola crassifolia
Scaevola gaudichaudiana
Ageratina adenophora
Fagraea cuspidata
Strychnos ignatii
Tabernaemontana sp
Alyxia stellata
Urophyllum glabrum
Psychotria mariniana
Coprosma longifolia
Hedyotis terminalis
Hedyotis acuminata
Hedyotis forbergii
Ludekia borneensis
Neonauclea artocarpioides
Uncaria cordata
Bobea elatior
Ixora grandifolia
Psydrax odorata
Coffea arabica
Cestrum nocturnum
Olea europaea
Chionanthus pluriflorus
Fraxinus excelsior
Fraxinus angustifolia
Citharexylum caudatum
Lantana camara
Jacaranda copaia
Tabebuia rosea
Buddleja davidii
Gmelina arborea
Clerodendrum macrostegium
Callicarpa longifolia
Abies borisii-regis
Abies alba
Pseudotsuga menziesii
Larix decidua
Picea sitchensis
Picea abies
Pinus cembra
Pinus canariensis
Pinus brutia
Pinus pinaster
Pinus halepensis
Pinus pinea
Pinus nigra
Pinus mugo
Pinus sylvestris
Pinus contorta
Pinus taeda
Pinus radiata
Juniperus oxycedrus
Juniperus thurifera
Araucaria columnaris
Podocarpus neriifolius
Conostylis candicans
Hedychium flavescens
Etlingera brevilabrum
Piper aduncum
Eusideroxylon zwageri
Cinnamomum burmanni
Cinnamomum zeylanicum
Persea americana
Maasia sumatrana
Popowia pisocarpa
Uvaria sassandrensis
Goniothalamus uvarioides
Grevillea robusta
Helicia attenuata
Banksia menziesii
Banksia sessilis
Leea indica
Pelargonium capitatum
Combretum nigrescens
Melastoma malabathricum
Clidemia hirta
Miconia pyrifolia
Melaleuca systena
Melaleuca leuropoma
Melaleuca quinquenervia
Pimenta dioica
0.022
trait value
0.329
length=176.162

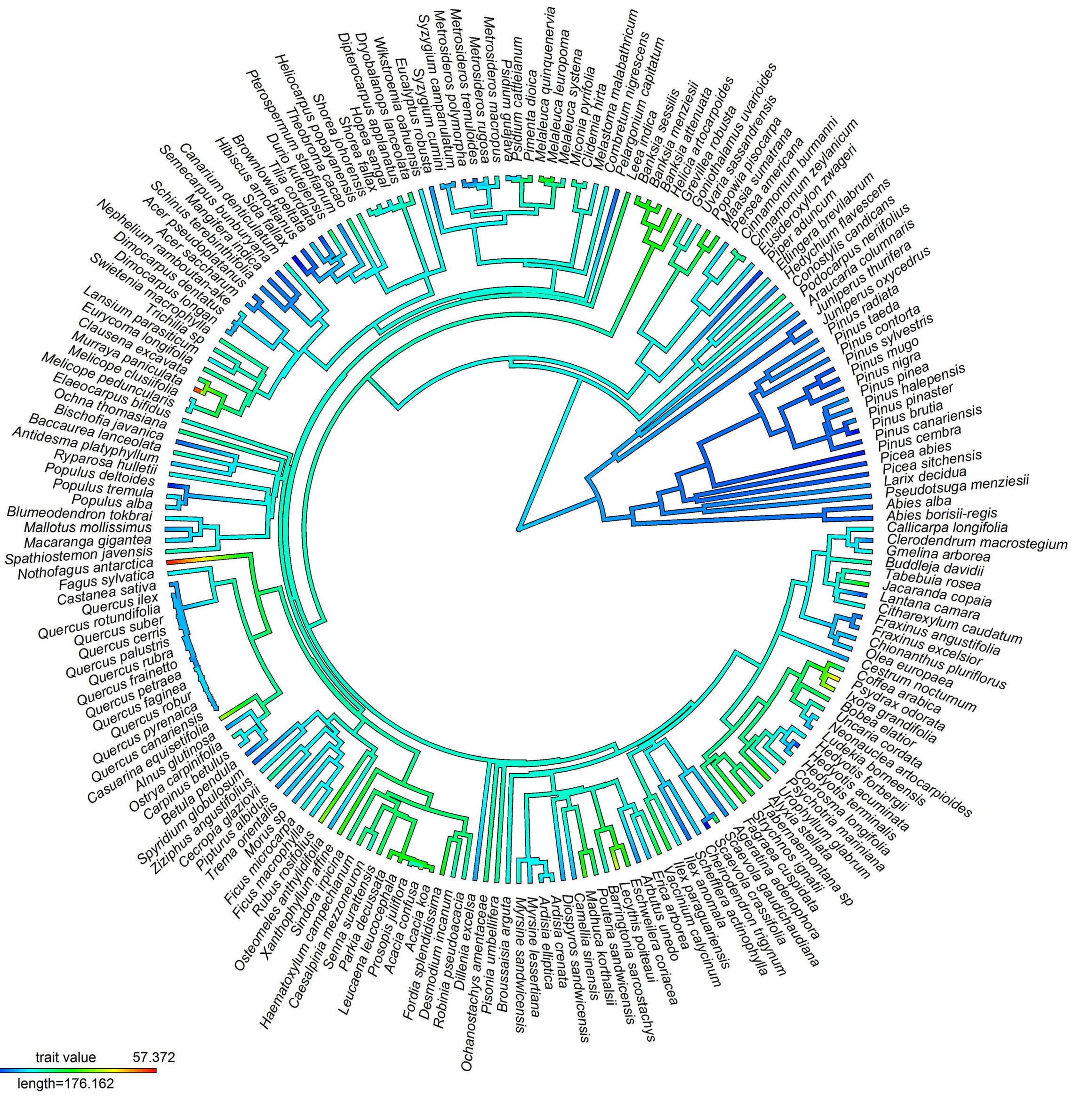
Metrosideros macropus
Metrosideros rugosa
Metrosideros tremuloides
Metrosideros polymorpha
Syzygium campanulatum
Syzygium cumini
Syzygium robusta
Eucalyptus oahuensis
Wikstroemia lanceolata
Dryobalanops applanatus
Dipterocarpus hasseltii
Hopea sangal
Shorea johorensis
Shorea faguetiana
Heliocarpus popayanensis
Theobroma cacao
Pterospermum stapfianum
Durio kutejensis
Tilia cordata
Brownlowia peltata
Hibiscus arnottianus
Sida fallax
Canarium denticulatum
Mangifera indica
Semecarpus bunburyana
Schinus terebinthifolia
Acer pseudoplatanus
Acer saccharum
Nephelium ramboutan-ake
Dimocarpus dentatus
Dimocarpus longan
Swietenia macrophylla
Trichilia sp
Lansium parasiticum
Eurycoma longifolia
Clausena excavata
Murraya paniculata
Melicope clusiifolia
Melicope peduncularis
Elaeocarpus bifidus
Ochna thomasiana
Bischofia javanica
Baccaurea lanceolata
Antidesma platyphyllum
Ryparosa hulletii
Populus deltoides
Populus tremula
Populus alba
Blumeodendron tokbrai
Mallotus mollissimus
Macaranga gigantea
Spathiostemon javensis
Nothofagus antarctica
Fagus sylvatica
Castanea sativa
Quercus ilex
Quercus rotundifolia
Quercus suber
Quercus cerris
Quercus palustris
Quercus rubra
Quercus frainetto
Quercus petraea
Quercus faginea
Quercus robur
Quercus pyrenaica
Quercus canariensis
Casuarina equisetifolia
Alnus glutinosa
Ostrya carpinifolia
Carpinus betulus
Betula pendula
Spyridium globulosum
Ziziphus angustifolius
Cecropia glaziovii
Pipturus albidus
Morus sp
Trema orientalis
Ficus microcarpa
Ficus macrophylla
Rubus rosifolius
Osteomeles anthylidifolia
Xanthophyllum affine
Haematoxylum campechianum
Sindora irpicina
Caesalpinia mezzoneuron
Senna surattensis
Parkia decussata
Leucaena leucocephala
Prosopis juliflora
Acacia confusa
Acacia koa
Fordia splendidissima
Desmodium incanum
Robinia pseudoacacia
Dillenia excelsa
Ochanostachys amentaceae
Pisonia umbellifera
Broussaisia arguta
Myrsine sandwicensis
Myrsine lessertiana
Ardisia elliptica
Ardisia crenata
Diospyros sandwicensis
Camellia sinensis
Madhuca korthalsii
Pouteria sandwicensis
Barringtonia racemosa
Lecythis poiteaui
Eschweilera coriacea
Arbutus unedo
Erica arborea
Vaccinium calycinum
Ilex paraguariensis
Ilex anomala
Scheffflera actinophylla
Cheirodendron trigynum
Scaevola crassifolia
Scaevola gaudichaudiana
Ageratina adenophora
Fagraea cuspidata
Strychnos ignatii
Tabernaemontana sp
Alyxia stellata
Urophyllum glabrum
Psychotria mariniana
Coprosma longifolia
Hedyotis terminalis
Hedyotis acuminata
Hedyotis forbergii
Ludekia borneensis
Neonauclea artocarpioides
Uncaria cordata
Bobea elatior
Ixora grandifolia
Psydrax odorata
Coffea arabica
Cestrum nocturnum
Olea europaea
Chionanthus pluriflorus
Fraxinus excelsior
Fraxinus angustifolia
Citharexylum caudatum
Lantana camara
Jacaranda copaia
Tabebuia rosea
Buddleja davidii
Gmelina arborea
Clerodendrum macrostegium
Callicarpa longifolia
Abies borisii-regis
Abies alba
Pseudotsuga menziesii
Larix decidua
Picea sitchensis
Picea abies
Pinus cembra
Pinus canariensis
Pinus brutia
Pinus pinaster
Pinus halepensis
Pinus pinea
Pinus nigra
Pinus mugo
Pinus sylvestris
Pinus contorta
Pinus taeda
Pinus radiata
Juniperus oxycedrus
Juniperus thurifera
Araucaria columnaris
Podocarpus neriifolius
Conostylis candicans
Hedychium flavescens
Etlingera brevilabrum
Piper aduncum
Eusideroxylon zwageri
Cinnamomum zeylanicum
Cinnamomum burmanni
Persea americana
Maasia sumatrana
Popowia pisocarpa
Uvaria sassandrensis
Goniothalamus uvarioides
Grevillea robusta
Helicia attenuata
Banksia menziesii
Banksia sessilis
Leea indica
Pelargonium nigrescens
Combretum malabathricum
Melastoma malabathricum
Clidemia hirta
Miconia pyrifolia
Melaleuca systena
Melaleuca leuropoma
Melaleuca quinquenervia
Pimenta dioica
Psidium cattleianum
Psidium guajava
3.723
trait value
57.372
length=176.162

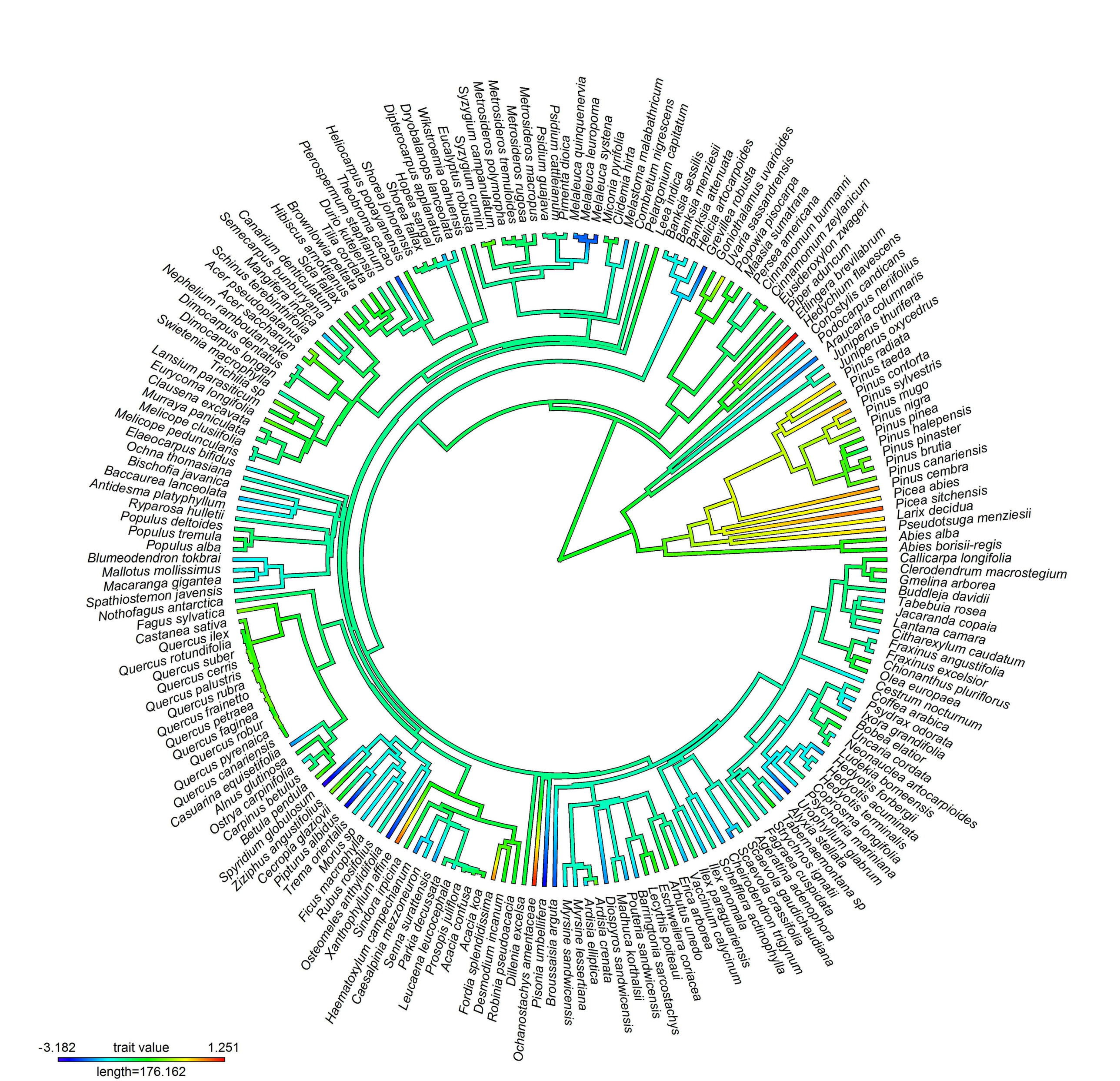
Psidium cattleianum
Psidium guajava
Metrosideros macropus
Metrosideros rugosa
Metrosideros tremuloides
Metrosideros polymorpha
Syzygium campanulatum
Syzygium cumini
Syzygium robusta
Eucalyptus oahuensis
Wikstroemia lanceolata
Dryobalanops applanatus
Dipterocarpus hasseltii
Hopea sangal
Shorea johorensis
Shorea faguetiana
Theobroma cacao
Heliocarpus popayanensis
Durio kutejensis
Pterospermum stapfianum
Tilia cordata
Brownlowia peltata
Hibiscus arnottianus
Sida fallax
Canarium denticulatum
Semecarpus bunburyana
Mangifera indica
Schinus terebinthifolia
Acer pseudoplatanus
Acer saccharum
Nephelium ramboutan-ake
Dimocarpus dentatus
Dimocarpus longan
Swietenia macrophylla
Trichilia sp
Lansium parasiticum
Eurycoma longifolia
Clausena excavata
Murraya paniculata
Melicope clusiifolia
Melicope pedunculariis
Elaeocarpus bifidus
Ochna thomasiana
Bischofia javanica
Baccaurea lanceolata
Antidesma platyphyllum
Ryparosa hulletii
Populus deltoides
Populus tremula
Populus alba
Blumeodendron tokbrai
Mallotus mollissimus
Macaranga gigantea
Spathiostemon javensis
Nothofagus antarctica
Fagus sylvatica
Castanea sativa
Quercus ilex
Quercus rotundifolia
Quercus suber
Quercus cerris
Quercus palustris
Quercus rubra
Quercus frainetto
Quercus petraea
Quercus faginea
Quercus robur
Quercus pyrenaica
Quercus canariensis
Casuarina equisetifolia
Alnus glutinosa
Ostrya carpinifolia
Carpinus betulus
Betula pendula
Spyridium globulosum
Ziziphus angustifolius
Cecropia glaziovii
Pipturus albidus
Morus sp
Trema orientalis
Ficus macrophylla
Rubus rosifolius
Osteomeles anthyllidifolia
Xanthophyllum affine
Sindora irpicina
Haematoxylum campechianum
Caesalpinia mezzoneuron
Senna surattensis
Parkia decussata
Leucaena leucocephala
Prosopis juliflora
Acacia confusa
Acacia koa
Fordia splendidissima
Desmodium incanum
Robinia pseudoacacia
Dillenia excelsa
Ochanostachys amentaceae
Pisonia umbellifera
Broussaisia arguta
Myrsine sandwicensis
Myrsine lessertiana
Ardisia elliptica
Ardisia crenata
Diospyros sandwicensis
Madhuca korthalsii
Pouteria sandwicensis
Barringtonia sarcostachys
Lecythis poiteaui
Eschweilera coriacea
Arbutus unedo
Erica arborea
Vaccinium calycinum
Ilex paraguariensis
Ilex anomala
Scheffiera actinophylla
Cheirodendron trigynum
Scaevola crassifolia
Scaevola gaudichaudiana
Ageratina adenophora
Fagraea cuspidata
Tabernaemontana sp
Strychnos ignatii
Alyxia stellata
Urophyllum glabrum
Psychotria mariniana
Coprosma longifolia
Hedyotis terminalis
Hedyotis acuminata
Hedyotis forbergii
Ludekia borneensis
Neonauclea artocarpioides
Uncaria cordata
Bobea elatior
Ixora grandifolia
Psydrax odorata
Coffea arabica
Cestrum nocturnum
Olea europaea
Chionanthus pluriflorus
Fraxinus excelsior
Fraxinus angustifolia
Citharexylum caudatum
Lantana camara
Jacaranda copaia
Tabebuia rosea
Buddleja davidii
Gmelina arborea
Clerodendrum macrostegium
Callicarpa longifolia
Abies borisii-regis
Abies alba
Pseudotsuga menziesii
Larix decidua
Picea sitchensis
Picea abies
Pinus cembra
Pinus canariensis
Pinus brutia
Pinus pinaster
Pinus halepensis
Pinus pinea
Pinus nigra
Pinus mugo
Pinus sylvestris
Pinus contorta
Pinus taeda
Pinus radiata
Juniperus oxycedrus
Juniperus thurifera
Araucaria columnaris
Podocarpus neriifolius
Conostylis candicans
Hedychium flavescens
Etlingera brevilabrum
Piper aduncum
Eusideroxylon zwageri
Cinnamomum zeylanicum
Cinnamomum burmanni
Persea americana
Maasia sumatrana
Popowia pisocarpa
Uvaria sassandrensis
Goniothalamus uvarioides
Grevillea robusta
Helicia attenuata
Banksia menziesii
Banksia sessilis
Leea indica
Pelargonium capitatum
Combretum nigrescens
Melastoma malabathricum
Clidemia hirta
Miconia pyrifolia
Melaleuca systena
Melaleuca leuropoma
Melaleuca quinquenervia
-3.182
trait value
1.251
length=176.162

Loadings

Scores

Quercus ilex

Pinus pinaster

[K]

Quercus petraea

[N]

[S]

[P]

[Ca]

Quercus robur

Pinus halepensis

[Mg]

Root 2 (5.0%)

Root 1 (90.8%)

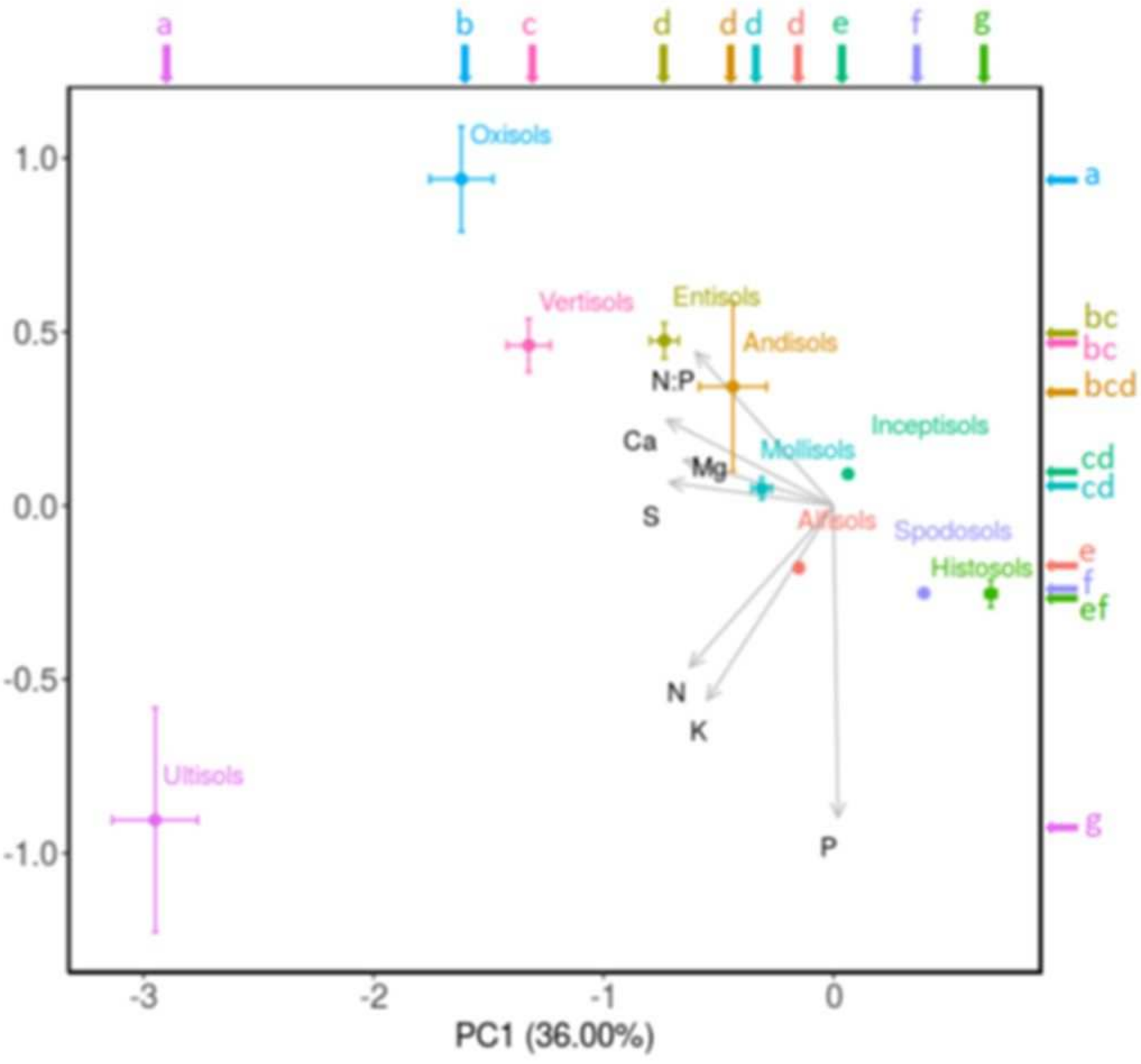
a
b
c
d
d d
d
e
f
g
Oxisols
1.0
0.5
0.0
-0.5
-1.0
PC2 (23.04%)
Vertisols
Entisols
Andisols
N:P
Ca
Mg
S
Mollisols
Inceptisols
Alfisols
Spodosols
Histosols
N
K
P
Ultisols
-3
-2
-1
0
PC1 (36.00%)
a
bc
bc
bcd
cd
cd
e
f
ef
g